

REVIEW

[View Article Online](#)
[View Journal](#) | [View Issue](#)



Cite this: *Ind. Chem. Mater.*, 2026, 4, 7

Electrooxidation of alcohols under the operating conditions of industrial alkaline water electrolysis

Floris van Lieshout, ^a Eleazar Castañeda-Morales, ^b
Arturo Manzo-Robledo ^b and Dulce M. Morales *^a

Hydrogen generation through conventional water electrolysis (CWE) is becoming increasingly prevalent on an industrial scale. However, widespread implementation is partially hampered by the sluggish kinetics of the oxygen evolution reaction (OER) and the severe (energy) costs associated with it. The electrooxidation of alcohols has received great interest within the scientific community as a potential alternative to the OER, leading to the emergence of a novel field known as hybrid water electrolysis (HWE). Nevertheless, while many efforts have been made by multiple stakeholders to give direction to CWE research with the aim of boosting its widespread industrial implementation, the same cannot be said for HWE. In this work, we provide an overview of target performance indicators for industrial alkaline CWE, and we discuss the extent to which the alcohol oxidation reaction (AOR), conducted under similar conditions, reaches those targets. Furthermore, we identify and discuss additional targets required for industrial application of HWE, with specific sections dedicated to the topics of selectivity and circularity of HWE products. In addition to this, we discuss the role that effective reactor design has in combating challenges associated with upscaling of HWE, followed by a description of novel approaches used in the literature. Finally, recommendations are given aiming to direct future research efforts towards industrial application of the AOR with simultaneous hydrogen production.

Received 4th May 2025,
Accepted 1st July 2025

DOI: 10.1039/d5im00071h

rsc.li/icm

Keywords: Electrolysis; Alcohol electrooxidation; Alkaline water electrolysis; Hybrid water electrolysis; Industrially relevant conditions.

1 Introduction

A sustainable and abundant source of green hydrogen has been regarded as an essential component in the current technological efforts to decarbonize refining, transportation and energy-related industries.^{1,2} Particularly, it has become urgent to reduce the harmful environmental impact of well-established industrial processes that depend on the use of large amounts of hydrogen, typically sourced from steam reforming, such as the Haber-Bosch process. Furthermore, emerging technologies such as direct CO₂ hydrogenation³ or Fischer-Tropsch synthesis⁴ will require an abundant stream of green hydrogen to become feasible green alternatives to current fossil-based sources. While the Sustainable Development Goals, established in 2015 by the United Nations, address these needs,⁵ they are often in conflict with the financial feasibility of alternative, environmentally-

friendly processes. This is well reflected in the price discrepancy between green hydrogen and its environmentally harmful counterparts, such as grey or blue hydrogen, which involve the co-generation of CO₂ in their production.⁶

Globally, green hydrogen represents only about 4% of the total hydrogen production.⁷ The low market for green hydrogen could be associated to its low price-competitiveness compared to hydrogen produced *via* fossil fuel-based methods, such as steam reforming, which emit seven times the amount of CO₂ per kilogram of hydrogen generated.⁸ Currently, there is a sizeable research momentum behind the industrial deployment of large-scale water electrolyzers to reduce the previously mentioned price discrepancy and meet sustainability targets. These efforts are primarily focused on scaling up lab-scale water electrolysis to an industrial level while maintaining a sufficiently high energy and cost efficiency.⁹ This transition is promoted by large intergovernmental organizations, such as the International Renewable Energy Agency (IRENA) and the European Clean Hydrogen Partnership (ECHP), which have set out technical targets for the next 25 years to achieve widespread industrial adoption of water electrolysis.^{2,10} Despite these efforts, conventional water electrolysis (CWE, Fig. 1a) still faces

^aEngineering and Technology Institute Groningen (ENTEG), University of Groningen, Nijenborgh 3, Groningen, 9747 AG, The Netherlands.

E-mail: d.m.morales.hernandez@rug.nl

^bInstituto Politécnico Nacional, Laboratorio de electroquímica y corrosión, Escuela Superior de Ingeniería Química e Industrias Extractivas, Unidad Profesional Adolfo López Mateos, Av. Instituto Politécnico Nacional S/N, CDMX, 07708 Mexico



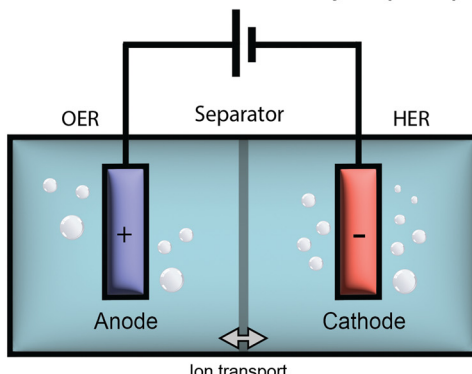
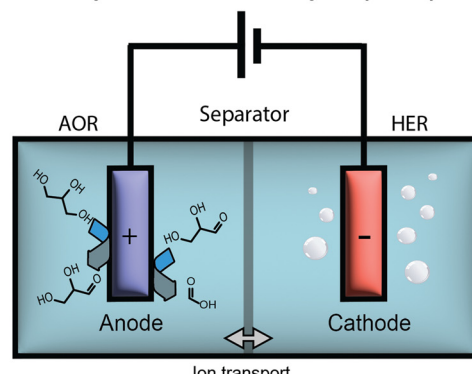
a Conventional water electrolysis (CWE)**b Hybrid water electrolysis (HWE)**

Fig. 1 Schematic illustration of (a) conventional water electrolysis and (b) hybrid water electrolysis.

challenges. Particularly, the anode process, the oxygen evolution reaction (OER), has been identified as the main bottleneck in terms of energy efficiency for industrial implementation this technology due to its sluggishness and the difficulty to achieve long-term stability with highly active electrocatalytic materials.¹¹ Hybrid water electrolysis (HWE) has been recognized in recent years as an approach to remediate some of the shortcomings of CWE.¹² In a hybrid water electrolyzer, a reaction alternative to the OER takes place at the anode, usually the electrooxidation of an organic compound (Fig. 1b, right), enabling thereby the following advantages:

- *Saving energy*: the electrooxidation of organic compounds, such as low-weight alcohols has shown to be thermodynamically more favorable than the more energy-intensive OER which occurs at 1.23 V vs. RHE.^{13,14} Replacing the OER by such alternative anode reaction translates into a decrease in the cell voltage required for the overall process, and an increment in the energy conversion efficiency for hydrogen production (see section 2.2). Furthermore, it has been reported that these benefits can be obtained using catalytic materials based on earth-abundant metals, such as nickel and cobalt, for electrolysis in alkaline media.^{15,16}

- *Inhibition of the OER*: it has been shown that under certain conditions, the alcohol oxidation reaction (AOR) may partially or completely inhibit the OER.¹⁷ Implementing this reaction in a HWE provides the possibility of circumventing one of the greatest safety risks associated with CWE, namely, H₂ and O₂ crossover through a membrane or separator, from which explosive mixtures can be formed.¹⁸

- *Production of valuable chemicals*: the partial oxidation of organic compounds, including low-cost alcohols, can result in the formation of value-added products of commercial interest, potentially increasing the economical attractiveness of the electrolytic process as a whole in addition to the production of green hydrogen.¹⁹ Furthermore, the alcohol substrates can often be sourced from waste streams. An example of such a compound is glycerol, originating as a large side stream from the transesterification reaction used for the production of biodiesel.²⁰ Another example is ethanol,

which can be produced through fermentation of biomass.²¹ A vast array of “small molecule” oxidation reactions have been shown to produce hydrogen with relatively high energy efficiency with concurrent generation of value added products.^{22,23}

- *Greenhouse gas (GHG) reduction efficiency*: it has been shown that, if HWE is optimized on a process level, its ability to reduce GHG emissions per MWh of electricity invested is almost twice the amount when compared to CWE. This feature will elevate HWE on the priority list for the allocation of the scarce resource, renewable electricity.²⁴

With these shortcomings remediated, HWE could prove industrially interesting. Despite this, limited research has been devoted to investigating HWE under the operating conditions that are relevant for industrial water electrolysis in alkaline media. Furthermore, it could be the case that the industrially relevant conditions for HWE differ from those of CWE; however, to the best of our knowledge, no attempt has been made at gauging what these conditions could be.

Herein, we address this knowledge gap by reviewing recent literature on HWE, specifically concerning the oxidation of alcohols as anode process, investigated under conditions that are relevant for industrial water electrolysis in alkaline media. In section 2, we provide an overview of the mentioned conditions, which are set as targets for industrial CWE, and are related to three key parameters: i) the current density requirements (with their associated overpotentials and voltages), ii) the operating temperature and iii) the electrolyte composition. By drawing parallels with targeted industrial conditions set out for CWE in alkaline media, an overview is provided on the feasibility of implementing the HWE under similar conditions. Recognizing the complexity that an alternative anode reaction brings to the process, the challenges inherent to HWE (including the need to achieve high selectivity and circularity) are discussed in section 3. Further, in section 4, we discuss the possibilities of enhancing the applicability of HWE through reactor and process design as reported in the literature. Lastly, a summary is provided in section 5 which functions as an



outlook for industrial application of HWE and provides recommendations to give direction for future research on HWE.

2 HWE under the target conditions for industrial water electrolysis in alkaline media

In this section, the current state of the art concerning industrial CWE will be discussed, along with goals for future improvements set by notable stakeholders such as IRENA and ECHP. Considering both the present advancements and the future trajectory of industrial CWE, including their key performance indicators (KPIs), studies performing HWE under similar conditions will be examined.

2.1 Target conditions for alkaline water electrolysis

In recent literature concerning CWE technology, increasing attention has been paid to industrial applicability.^{9,25-27} This has resulted in collective efforts to define current and future performance targets. Examples of these efforts can be found in the IRENA report concerning the reduction of green hydrogen cost² and in the Strategic Research and Innovation Agenda defined by the ECHP.¹⁰ In these reports, targets are set for relevant KPIs such as current density, voltage, temperature, stability and system efficiency. These targets are meant to serve as a benchmark and thereby provide guidance for future research. Therefore, in this section an overview of the targets set for CWE are summarized (Fig. 2), focusing in particular on (i) current density and voltage, (ii) electrolyte composition, and (iii) operating temperature. It is important to mention that there are additional, highly relevant targets related to long-term performance, energy consumption and cell pressure. However, these are out of the scope of this review due to the limited number of reports that address these in the context of the AOR or of HWE.

1) Current density and voltage. During an electrolysis process, the electrochemical cell requires more energy than

what is thermodynamically expected to drive each of the half-reactions. This additional energy is known as overpotential (η). It is often determined from voltammetric experiments at a certain current density to evaluate and compare the activity of electrocatalytic materials towards certain half-reaction, including the OER.²⁸ Eqn (1) gives a relation between η and the electrode potential (E) of a reaction,

$$E = E^\circ + \eta + iR \quad (1)$$

where E° is the standard potential of the electrochemical reaction, and iR is the ohmic drop in the electrode potential due to the current flowing (i) and the (uncompensated) resistance (R).²⁹ The voltage that is required to run the reaction is the difference in the electrode potentials of the two half-reactions, and, therefore, a combination of all the previously mentioned variables, including the overpotentials. Moreover, the overpotential is influenced by parameters such as the electrode surface area (A), the nature and quality of the electrode films, the reactor geometry, the electrolyte composition and the operating conditions, in addition to the electrocatalytic capabilities of a given electrode material. In a large-scale water electrolyzer, the high overpotentials required to reach the targeted current densities lead to various issues,³⁰ such as:

- *Increased energy consumption:* the energy supplied is not efficiently used for the desired reaction, related partly to energy losses in the form of heat, which in turn increases the operational costs.

- *Side reactions:* high overpotentials imply that it is necessary to apply higher voltages to the electrochemical system, which can induce unwanted side reactions that compete with the main electrooxidation process, limiting its efficiency and selectivity.

- *Reduced hydrogen production efficiency:* a high overpotential translates into a limitation in the reaction rate at the cathode, thus decreasing the overall hydrogen output. This also means that larger cell sizes are required to achieve a desired production rate, affecting the compactness of the electrolyzer and increasing the associated costs.



Fig. 2 A timeline of the technical advancements related to alkaline water electrolysis proposed by the International Renewable Energy Agency (IRENA),² the Joint Hydrogen Undertaking (JHU) developed by European Clean Hydrogen Partnership (ECHP),¹⁰ and an overview of the state of the art as given by the JHU and IRENA in 2020. *Degradation is defined here as the energy efficiency loss when running at nominal capacity for a given time.



In CWE, a prime focus resides in the energy efficiency of the process, *i.e.*, what input voltage must be applied to reach a certain current density. For many years, the performances of OER catalysts were typically evaluated based on their overpotential at a current density of 10 mA cm^{-2} , proposed as a benchmark methodology in 2013,³¹ which corresponds to a 10% efficient solar-to-fuel conversion device. However, it has been shown that this figure is often not representative of the performance at higher current densities. Considering the reports by IRENA and the ECHP for alkaline water electrolysis, state-of-the-art nominal current densities are in the range between 0.2 and 0.8 A cm^{-2} at an input voltage between 1.4 and 3 V, which renders evaluations done at 10 mA cm^{-2} insufficient to assess the industrial applicability of electrocatalytic materials. Looking into the future, IRENA has set the target of reaching a current density above 2 A cm^{-2} at an input voltage lower than 1.7 V by 2050. Considering that this is a challenging goal for the immediate future, the ECHP proposed a target to 1 A cm^{-2} for 2030. Taking into account that these are optimistic targets set for a much more mature CWE technology, HWE systems could be considered industrially relevant at this time since its current densities already approach the ampere-level ($0.3\text{--}1.0 \text{ A cm}^{-2}$) at an input of less than 2 V. This is reviewed in detail in section 2.2. Furthermore, an important industrial parameter to consider is stability, with ambitious goals of roughly 100 000 h of continuous operation with minimal degradation being targeted by IRENA. As several factors, including electrode potential, operating temperature and electrolyte composition, affect the stability, this will be discussed throughout the review in sections specifically dedicated to these. In section 2.2, we cover reports on the AOR that target industrially relevant current densities at low overpotentials.

2) **Electrolyte composition.** In typical lab-scale investigations, performance evaluation of electrocatalytic materials for alkaline water electrolysis is conducted in KOH or NaOH solutions of concentrations ranging between 0.1 and 1 M. A more concentrated electrolyte solution increases the conductivity, which is beneficial for energy conversion efficiency. Currently, most industry-scale alkaline water electrolyzers operate with KOH concentrations in the range from 5 to 7 M.² No specific targets for the variation of electrolyte or the concentration have been proposed in the previously mentioned reports. However, it is important to note that this variable has a direct impact on the operating voltage, since larger overpotentials are required to overcome the ohmic resistances arising from conductivity limitations. For HWE, it is particularly important to consider this since the addition of an organic compound may lead to a substantial increase in the solution resistance, but a very small low concentration will lead to other challenges related to downstream separation. In addition to this, the (electro)chemical stability of organic compounds as well as the employed electrocatalysts depend

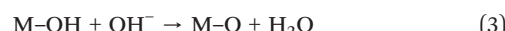
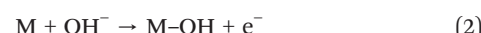
strongly on the electrolyte composition. In section 2.3, we discuss AOR experiments conducted in strongly alkaline electrolytes with variable concentration conditions. Furthermore, reports concerning the concentration effect of the alcohol in turn on the observed electrocatalytic performance are discussed.

3) **Operating temperature.** Conducting electrolysis at elevated temperatures is beneficial for CWE operation, as the thermal energy can replace, to a certain extent, the excess of electrical energy required. This energy can be sourced from waste heat streams.³² In addition to this, reactions also benefit from enhanced kinetics at higher temperatures. The typical temperature operation window for CWE is in the range from 70 to 90 °C, with operation targets set by IRENA for >90 °C in the future. In this review, we cover reports that investigate the AOR at temperatures above room temperature, see section 2.4.

2.2 Overpotential and current density

A high overpotential induces negative consequences for industrial electrolyzers, decreasing the energy efficiency while increasing the production and maintenance costs, and thus it hinders possibilities for practical application and scalability. Substituting the kinetically sluggish OER process with a thermodynamically more favorable electrooxidation process, such as the AOR (Fig. 3), affords an innovative and energy-saving hydrogen production method. Concisely, to reach the same current density, the AOR requires low overpotentials compared to the OER, thus overcoming several of the issues mentioned earlier.^{17,33}

During the electrolysis processes, intermediates are formed on the catalyst surface. Their associated Gibbs energy of adsorption/desorption give rise to different energy barriers.³⁴ The reaction mechanisms proposed for the OER in alkaline media involve OH^- ions, which are adsorbed on the catalytic sites (M) to form M-OH species, thereby donating one electron (eqn (2)). Another OH^- ion is adsorbed on the M-OH site, forming M-O (eqn (3)), and leading to two different pathways to form O_2 : 2M-O produces O_2 leaving 2M sites available (eqn (4)), or M-O is converted to the M-OOH intermediate by reacting with OH^- (eqn (5)), with a fourth OH^- ion reacting with the formed M-OOH species to form O_2 and H_2O , and transferring one electron (eqn (6)).³⁵ The kinetics of these reactions can be modulated by varying the nature of the catalytic site, the pH (or OH^- concentration) and/or the operating temperature.³⁶



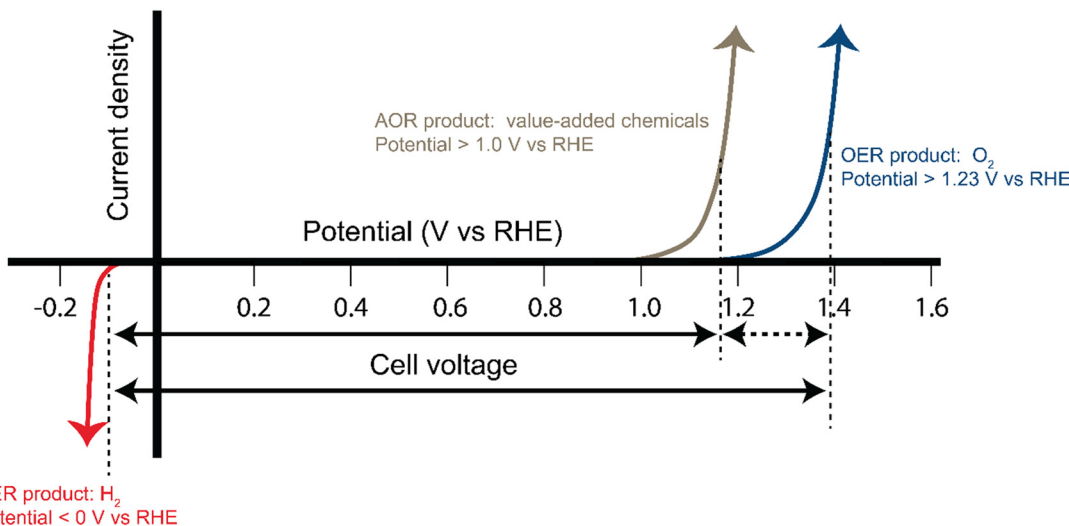
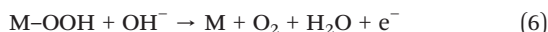
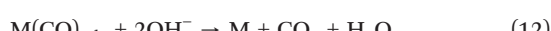


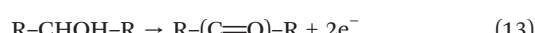
Fig. 3 Energy requirements and products of the hydrogen evolution reaction (HER), the alcohol oxidation reaction (AOR) and the oxygen evolution reaction (OER).



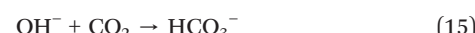
More complex than the OER, the AOR involves the formation of several intermediates following various pathways. In general, the partial electrooxidation of alcohols in alkaline media results in the formation of aldehydes/ketones and carboxylates. The complete oxidation reaction of a primary alcohol is exemplified for methanol in the following.³⁷ This oxidation pathway requires the initial adsorption of an alcohol molecule on the catalyst surface (seen in eqn (7)), followed by the dehydrogenation of the hydroxyl group (eqn (8)). Subsequently the hydrogens attached to the carbon in the alcohol group are released dissociating the C-H bonds (eqn (8)–(10)). That step is repeated to obtain adsorbed CO molecule on the catalyst surface and it is then oxidized to CO₂ (eqn (11) and (12)). It should be noted that the precise mechanism of the AORs is still under investigation, for this we refer the reader to a specialized review for a more in-depth discussion of proposed AOR mechanisms.³⁸



From the electrooxidation of secondary alcohols, carbonyl-derived groups can be formed (eqn (13)).



The product obtained from the full electrooxidation of alcohols is CO₂ (eqn (12)), which is rapidly converted to carbonate (CO₃²⁻) and bicarbonate (HCO₃⁻) species in alkaline conditions as shown in eqn (14) and (15).³⁹ While the presence of these species implies a constraint for electrochemical devices due to the precipitation of solid carbonate crystals that may partially block the electrode and membrane, thereby reducing the electrolyzer performance, this also offers a route towards CO₂ capture, which can be exploited for its further conversion to value-added chemicals.^{40,41} Tailoring reactor design to the specific needs of the AOR will be further discussed in section 4, including issues related to carbonate/bicarbonate formation.



Materials based on earth-abundant components, particularly transition metals such as Ni and Co, have proved to be promising alternatives to the scarce and expensive noble metals as catalysts for the AOR in alkaline media.⁴² A general mechanism for electrooxidation for primary alcohols on nickel surface in alkaline conditions was proposed by Fleischmann and coworkers.⁴³ Initially, nickel hydroxide (Ni(OH)₂), which is formed rapidly when metallic nickel is immersed in an alkaline electrolyte,⁴⁴ is oxidized to nickel oxyhydroxide (NiOOH, eqn (16)) with a change of the chemical state of nickel from Ni²⁺ to Ni³⁺. The formed NiOOH species induce the dehydrogenation of the alcohol. The interaction between the NiOOH and the alcohol allows the subsequent release of a hydrogen, and the reduction of NiOOH to Ni(OH)₂, as shown in eqn (17). Finally, the intermediates are oxidized forming carboxyl as seen in eqn (18).⁴⁵ It is generally accepted that the mechanism on the



cobalt surface is identical to that of the reaction at the nickel surface.³⁷



In the context of HWE, it is important to highlight that catalysts based on these transition metals have demonstrated a high activity towards the oxidation of numerous alcohols (including monoalcohols, diols and triols) in alkaline media, often exhibiting substantially lower overpotentials for the AOR than for the OER. Electrooxidation of primary alcohols usually takes place at anodic potentials above 1.40 V *vs.* the reversible hydrogen electrode (RHE) using transition metal-based materials as catalysts, particularly nickel.⁴⁶ The associated overpotentials depend largely on what alcohol is being oxidized. For instance, it has been demonstrated that the efficiency of nickel-modified graphite electrodes is higher for the AOR than for the OER in 1 M NaOH, achieving currents in the order methanol oxidation ($\sim 15 \text{ mA cm}^{-2}$) $>$ ethanol oxidation ($\sim 12 \text{ mA cm}^{-2}$) $>$ 1-propanol oxidation ($\sim 10 \text{ mA cm}^{-2}$) $>$ 2-propanol oxidation ($\sim 5 \text{ mA cm}^{-2}$) $>$ OER ($< 1 \text{ mA cm}^{-2}$) at 1.55 V *vs.* RHE, estimated from voltammetric data.⁴⁷ In another report, a material consisting of NiO_x nanoparticles supported on multiwalled carbon nanotubes (MWCNTs) was investigated as electrocatalyst for the oxidation of methanol, ethanol and glycerol in alkaline conditions (1 M KOH), showing an activity trend in the order glycerol oxidation $>$ ethanol oxidation $>$ methanol oxidation $>$ OER, according to cyclic voltammetry data.¹⁷ It was further shown that not only the electrolyte composition but also the heteroatom functionalities of the MWCNTs support have an important influence on the observed overpotentials as well as on the selectivity in terms of the competition between the OER and the AOR. In the case of the glycerol oxidation reaction (GOR), this same Ni-based catalyst achieved a decrease in overpotential of 280 mV with respect to the OER measured at 10 mA cm⁻², while analogous catalysts based on Co, Fe and Mn achieved lower decreases in overpotential of 130, 90 and 40 mV, respectively.⁴⁸ Similarly, in a report by Chen and coworkers, NiO particles exhibited current densities of 7.5 mA cm⁻² at an electrode potential of 1.64 V *vs.* RHE in the absence of any alcohol (OER), while it was 1.54 and 1.46 V *vs.* RHE in the presence of 50 mM ethanol or ethylene glycol, respectively.⁴⁹ Similar trends have been reported with other transition metals. For instance, the AOR activity of the $\text{Cu}_{80}\text{Co}_{20}$ hydroxycarbonate was analyzed, using as electrolyte 1 M KOH in the presence of 0.1 M ethanol, ethylene glycol or glycerol, and achieving current densities of 7.9, 23.4 and 40.4 mA cm⁻², respectively, at 1.6 V *vs.* RHE.¹⁵

In several of the aforementioned reports, the overpotentials required for the electrooxidation of diols or

triols are lower than those required for monoalcohols. However, this largely depends on the catalyst properties. For instance, during the electrooxidation of various alcohols on $\beta\text{-Ni(OH)}_2$ catalyst in 1 M KOH, current densities of 0.17, 0.22, 5.78 and 6.05 mA cm⁻² were measured at 1.5 V *vs.* RHE in the presence of 0.1 M 1,2-propanediol, ethylene glycol, 1-propanol and ethanol, respectively, demonstrating the highest current density in the presence of ethanol compared to other alcohols on this catalyst surface.⁵⁰ Brix and coworkers investigated a series of $\text{LaFe}_{1-x}\text{Co}_x\text{O}_3$ materials and demonstrated that the OER, the GOR and the ethanol oxidation reaction (GOR) could be favored differently depending on both the metal and phase composition.⁵¹ Thus, further decrease in overpotentials can be achieved by tuning the synthesis conditions, thus impacting the catalyst composition as well as their structural and electronic properties. For instance, Nacef and coworkers evaluated Ni films electrodeposited from solutions with different pH (3.8, 4.5 and 6.7) as catalysts for the GOR, and it was shown that at a deposition pH of 6.72, the resulting nickel film exhibited a lower overpotential (1.38 V *vs.* RHE at 20 mA cm⁻²) in comparison to the films deposited at lower pH values (1.48 and 1.69 V *vs.* RHE for pH 4.5 and 3.8, respectively, at the same current density), which was attributed to a decrease in the particle size at more alkaline conditions.⁵² In another recent report, nanoparticles of Ni, NiCu and NiCo were synthesized and evaluated as electrocatalysts for the GOR, requiring electrode potentials of 1.49, 1.41 and 1.25 V *vs.* RHE, respectively, to reach a current of 1 mA in an aqueous solution consisting of 1 M NaOH and 0.1 M glycerol.⁵³ Especially for the NiCo catalyst a 200 mV drop in potential was seen to achieve a 5 mA current for the GOR compared to the OER.

Catalysts support may also play a role in the overpotentials associated to the AOR. An example is found with a series of Ni_3Co_1 materials supported on different amounts of carbon nanotubes (CNT), which were evaluated as electrocatalysts for the oxidation of methanol and ethanol. The results showed that using an optimal CNT mass loading of 35% led to current densities of 213 and 181 mA cm⁻² at 1.79 V *vs.* RHE in the presence of 1 M of methanol and ethanol, respectively.⁵⁴ In another report, differential electrochemical mass spectrometry (DEMS) was used to monitor oxygen production during the AOR using Ni oxide nanoparticles supported on MWCNTs with and without N-doping. It was shown that the heteroatom functionalities of the MWCNTs support have an important influence on the selectivity of the oxidation of methanol, ethanol and glycerol, particularly, in terms of the competition between the OER and the AOR.¹⁷

Clearly, integrating the AOR as anode reaction can result in large decreases in overpotentials compared to the OER. Table 1 shows an overview of the difference between the overpotentials measured during the two anode reactions (ΔE_{anode}) for several reported electrocatalysts and electrolysis conditions. While this is advantageous in terms of energy efficiency, as discussed in section 2.1, not only low



Table 1 Overview of anodic potential differences (ΔE_{anode}), defined as the difference between oxygen evolution reaction potential (E_{OER}) and alcohol oxidation reaction potential (E_{AOR}), measured at the indicated current density for various noble metal-free electrocatalysts evaluated at room temperature in alkaline media

Catalyst	Electrolyte composition	E_{OER} (V vs. RHE)	E_{AOR} (V vs. RHE)	ΔE_{anode} (mV)	Ref.
Co _{0.4} NiS@NF	0.05 M HMF + 1 M KOH	1.70@200 mA cm ⁻²	1.31@200 mA cm ⁻²	390	55
NiMn-LDH	3 M MeOH + 1 M KOH	1.78@100 mA cm ⁻²	1.41@100 mA cm ⁻²	370	56
CoMoO ₄	0.1 M glycerol + 1 M KOH ^a	1.42@10 mA cm ⁻²	1.10@10 mA cm ⁻²	314	57
Ni(OH) ₂	0.1 M glycerol + 2 M LiOH	1.80@20 mA cm ⁻²	1.50@20 mA cm ^{-2a}	301	58
NiCo/CF	0.2 M BHMF + 1 M KOH	1.89 ^b @500 mA cm ⁻²	1.59 ^b @500 mA cm ⁻²	300	59
NiCo ₂ O ₄ /NF	0.1 M glycerol + 1 M KOH	1.64@50 mA cm ⁻²	1.34@50 mA cm ⁻²	299	60
NiO _x /MWCNTs-O _x	1 M glycerol + 1 M KOH	1.59@10 mA cm ⁻²	1.31@10 mA cm ⁻²	280	48
NiCo hydroxide	0.1 M glycerol + 1 M KOH	1.62 ^b @50 mA cm ⁻²	1.34@50 mA cm ⁻²	280	61
0.1Cu-Ni ₃ S ₂ @NF	0.5 M glycerol + 1 M KOH	1.69@100 mA cm ⁻²	1.41@100 mA cm ⁻²	280	62
Ni-Mo-N/CFC	0.1 M glycerol + 1 M KOH	1.57@10 mA cm ⁻²	1.30@10 mA cm ⁻²	270	63
Mn _{0.2} NiS/GF	0.1 M HMF + 1 M KOH	1.71@500 mA cm ⁻²	1.48@500 mA cm ⁻²	230	64
NiOOH-CuO	1.0 M EtOH + 1 M KOH	1.61@50 mA cm ⁻²	1.38@50 mA cm ⁻²	228	65
NiCo ₂ /NF	0.1 M glycerol + 1 M KOH	1.52@25 mA cm ⁻²	1.31@25 mA cm ⁻²	210	66
Ni-Co/CCE	0.1 M glycerol + 1 M NaOH	1.56 ^b @5 mA	1.76 ^b @5 mA	200	53
Ni(OH) ₂ /NF	0.5 M MeOH + 1 M KOH	1.52@100 mA cm ⁻²	1.36@100 mA cm ⁻²	160	67
Ni ₃ N/NM	0.1 M benzyl alcohol + 6 M KOH	1.47@400 mA cm ⁻²	1.32@400 mA cm ⁻²	150	27

Abbreviations: MWCNTs-O_x: oxidized multiwalled carbon nanotubes; CFC: carbon fiber cloth; NM: nickel mesh; NF: nickel foam; GF: graphite felt; LDH: layered double hydroxide; CF: cobalt foam; CCE: carbon cloth electrode.^a Performed at 60 °C. ^b Estimated from voltammograms.

overpotentials but also high current densities are targeted for industrial water electrolysis. However, literature reporting relevant current densities during the AOR is limited, and in very few cases values above 0.1 A cm⁻² have been reported (see Table 1). Considering that an operation target of >2 A cm⁻² was set for 2050,² the field of HWE could benefit of studies conducted at current densities of 0.5 A cm⁻² or higher, focusing not only on achieving low overpotentials but also catalyst stability and high selectivity (see section 3.1) under such operating currents.

2.3 Electrolyte composition

The activity and selectivity of electrocatalysts for the AOR can be strongly influenced by the composition of the electrolyte solution employed. In HWE, the solution in the anode compartment, namely the anolyte, consists usually of a mixture of an organic compound and an electrolyte solution. The latter presents the following characteristics: (i) it can be maintained in the liquid phase at the operating temperatures, (ii) it can dissolve the organic compound, and (iii) it is able to provide sufficient ionic conductivity for the electrolysis process.⁶⁸ The selection of the supporting electrolyte, typically a strong base such as KOH, has an important influence on the efficiency of the AOR. For instance, it has been shown that using bases with different cations may lead to changes in the electrocatalytic properties of anode materials, both in the presence and absence of an alcohol. In a report by Chodankar and coworkers, the OER performance of Ni₂P₂O₇ was evaluated in 2 M LiOH, NaOH and KOH solutions, showing that in KOH the catalyst exhibited a superior specific capacitance and current density for nickel oxidation due to factors such as electrical conductivity, solvation energy and ionic radii of species.⁶⁹ A

study on glycerol electrooxidation was carried out using electrodeposited Ni(OH)₂ as catalyst, evaluating its performance in 2 M of LiOH, NaOH, KOH and CsOH solutions in the presence of 0.1 M glycerol.⁵⁸ The results showed current densities of ~58, ~59, ~65, and ~76 mA cm⁻² measured at 1.6 V vs. RHE, corresponding to NaOH, LiOH, CsOH and KOH, respectively. The authors attributed the higher current density observed in K⁺ solution to the oxidative capability of adsorbed substrates on the catalyst surface, which was lower in the case of Li⁺ and the other small cations.

Another important factor to consider is the pH of the electrolyte. For instance, Liu and coworkers evaluated CuO as an electrocatalyst with 0.1 M NaOH (pH 13) and 0.1 M Na₂B₄O₇ (pH 9) as electrolyte in the presence of 0.1 M glycerol. The measured electrode potentials at 1 mA cm⁻² were significantly different: 1.38 and 1.83 V vs. RHE for NaOH and Na₂B₄O₇, respectively.⁷⁰ A similar study was conducted using Ni(OH)₂ as electrocatalysts for the GOR and electrolytes with pH values in the range from 9 to 13. A borate buffer was chosen for pH 9–12 with addition of K₂SO₄ to achieve similar concentration of K⁺ ions, and 0.1 M KOH was used for pH 13. The electrode potentials measured at a current density of 4 mA cm⁻² in the presence of 0.01 M glycerol were 1.81, 1.74, 1.78, 1.79 and 1.80 V vs. RHE corresponding to pH values of 13, 12, 11, 10 and 9, respectively. While there was no clear relation between the measured overpotentials and the pH of the electrolyte, it was demonstrated that the pH influences the Ni(OH)₂/NiOOH peak position (as observed in the absence of an alcohol), where higher pH values resulted on a shift of the peak to more positive potentials.¹⁶

KOH is the supporting electrolyte most commonly used for industrial alkaline water electrolysis, operating typically with KOH concentrations in the range from 25 to 30 wt% (5–



7 M).⁷¹ The use of highly alkaline electrolytes is associated with an enhancement of electrolyte conductivity, a larger availability of OH^- species (which can take part in the electrooxidation process), an increasing ability to form active alkoxide species, and an increment in the ionic transport.^{72,73} It is important to note that the ionic conductivity of the electrolyte increases with an increase in electrolyte concentration while increased coulombic interactions between the ions in the electrolyte decrease the conductivity. Optimal ionic conductivities for KOH are found in the concentration range between 5 and 8 M in a temperature range from 0 to 100 °C.⁷⁴ Despite this, there are only a few reports where the electrooxidation of alcohols were investigated in this range of alkaline conditions. For instance, Ni oxide supported on oxidized MWCNTs was evaluated as an electrocatalysts for the GOR in 1 and 7 M KOH solutions, observing electrode potentials of 1.31 and 1.28 V vs. RHE, respectively, at a current density of 10 mA cm^{-2} .⁴⁸ While the overpotential difference was only 30 mV, substantial differences in selectivity and product distribution were observed (this is discussed in detail in section 3.1). Another example is observed with the electrolysis of 8 M benzyl alcohol, using electrolyte solutions with different KOH concentrations (1, 2 and 5 M) and $\beta\text{-Ni(OH)}_2$ nanosheets as the electrocatalyst. The results revealed lower electrode potentials with higher KOH concentrations, achieving \sim 24, \sim 37 and \sim 67 mA cm^{-2} in 1, 2 and 5 M KOH, respectively, at a potential of 1.45 V vs. RHE.⁷⁵ Additionally, higher concentration (and thus alkalinity) of the supporting electrolyte can also lead to favorable changes in the properties of a catalyst. For instance, CuO/Cu supported on nickel foam (NiF) was tested as an electrocatalyst for the OER in three different KOH concentrations. Using 3 M KOH resulted in a more efficient change in the oxidation state of Cu compared to lower concentrations (0.5 and 1 M), associated to the formation of CuOOH which is the active Cu species towards electrooxidation of alcohols.⁷⁶ Another relevant example was reported by Ghosh *et al.* during the evaluation of nickel mesh (NM) coated with Ni_3N as an electrocatalysts for the oxidation of 0.1 M benzyl alcohol using 6 M KOH as electrolyte at an operating temperature of 85 °C, and obtaining an industrially relevant current density of 0.538 A cm^{-2} at 1.45 V vs. RHE.²⁷ Also in 6 M KOH solution, Ni_3B coated onto NF was evaluated as a catalyst for the electrooxidation of methanol (0.5 M), achieving an oxidation current of 62 A g^{-1} (\sim 155 mA cm^{-2}) at an electrode potential of 1.53 V vs. RHE.⁷⁷ As seen, employing highly concentrated KOH solutions might result in high current densities and/or low overpotentials. However, designing sufficiently stable materials that are electrochemically robust under these conditions remains a challenge.⁷⁸

To identify the optimal conditions for the alcohol oxidation process it is important to consider the concentration of the alcohol itself. For instance, copper bars were tested as electrocatalysts for the methanol oxidation

reaction (MOR) in 1 M KOH using methanol concentrations from 0.025 to 1 M. The results showed that an increase in the concentration of methanol causes a quasi-linear enhancement of the anodic currents.⁷⁹ A similar study was done on nickel/polydiphenylamine deposited onto fluorine-doped tin oxide (Ni/PDPA-FTO) evaluated in 0.1 M KOH with methanol concentrations from 0.5 to 2 M. It was found that the MOR peak current was enhanced as the alcohol concentration increased, translating in an increase in the oxidation rate.⁸⁰ In addition to influencing the current density, the alcohol concentration can also have an important effect on the measured overpotentials. For instance, Ni deposited onto three-dimensional porous graphene (Ni/3D-G) was evaluated as a MOR electrocatalyst using 1 M KOH solutions containing up to 2 M methanol. After increasing the methanol content, a marked shift of the anodic peak was observed, from 1.58 V vs. RHE in the alcohol-free solution to 1.36–1.41 V vs. RHE in the presence of methanol, depending on its concentration.⁸¹ Similar results were found with a NiCr-based catalyst tested in 1 M KOH solutions containing up to 3 M methanol. Remarkable changes in current densities were registered with increasing methanol content, increasing from 1 mA cm^{-2} for OER to 7 mA cm^{-2} at 3 M methanol both measured at 1.6 V vs. RHE.⁸² However, it is important to highlight that it is not always the case that a higher alcohol concentration results in a higher current density and/or a lower overpotential. The effect of the concentration of methanol and ethanol (0.05–1 M) was studied on a hetero-union $\text{MnO}_2\text{-NiO}/\text{MWCNTs}$ electrocatalyst. Optimal concentrations of 0.7 and 0.5 M were found for methanol and ethanol, respectively, while higher concentrations resulted in a decrease in the current density, which was attributed to the formation of alcohol oxidation (by)products saturating (or poisoning) the catalyst surface, preventing the adsorption of hydroxyl groups and, thus, disrupting the alcohol oxidation reactions.⁸³ Following this analysis, the GOR was carried out on a Ni/C catalyst surface varying the glycerol concentration from 0.005 to 0.1 M in 0.1 M KOH solutions. The relationship between current density and glycerol concentration indicated a deviation from linearity, seen as a plateau in the trend towards higher glycerol concentrations. This could be due to saturation of the NiOOH catalytic sites by a high glycerol content.⁸⁴ Such behavior was also observed during the oxidation of 2-propanol on a nickel surface tested in 1 M KOH with alcohol concentrations from 0.05 to 2 M. It was observed that the current density increases with an increase in 2-propanol concentration up to 0.5 M, while at higher concentrations (1 and 2 M) no further increase was evident.⁸⁵ Finally, it is also important to note that, with an increase in the alcohol concentration, the concentration of carbonaceous intermediates adsorbed onto the electrode surface is also higher, which can result in an inhibition of the OER. This was demonstrated by means of DEMS for glycerol, ethanol and methanol using a Ni-based catalyst.¹⁷



In summary, the electrolyte composition has a strong influence in the current densities and overpotentials associated to the electrooxidation of alcohols. As discussed above, this can be influenced by the nature and concentration of both the alcohol and the supporting electrolyte. A higher concentration of supporting electrolyte leads to a higher amount of free ion species (such as hydroxyl) in the solution, increasing the overall ionic conductivity of the electrolyte, and thus, until certain extent, increasing the current density and/or decreasing the overpotentials. However, in highly alkaline concentrations, other effects such as variations in the tolerance to alcohol oxidation intermediates and (by)products, an unfavorable competition between OH^- species and alcohol molecules for active sites, and insufficient electrochemical stability, could take place depending on the catalyst used. Systematic studies on the effect of using industry-like electrolytes for the AOR are still needed to draw conclusions. Concretely, electrolysis conducted in KOH concentrations near ~ 7 M at current densities above 0.1 A cm^{-2} are required to assess the potential implementation of the AOR as an alternative anode reaction for industrial water electrolysis, ideally involving a wide range of concentrations of different alcohols, and a wide variety of low-cost and scalable catalytic materials.

2.4 Operating temperature

The operating temperature plays a crucial role in every electrocatalytic process, influencing not only the thermodynamics of the reaction, but also the reaction kinetics, mass transport, conductivity, and stability of the electrocatalytic materials. These are discussed in the following.

- *Reaction kinetics:* with the increase of temperature, the reaction kinetics rises due to more frequent collisions between the species involved in the reaction. In other words, an increase in temperature leads to a higher reaction rate, which translates into a higher current density and, in the case of the AOR, a faster conversion of the alcohol.⁸⁶ This has been studied in reactions such as the EOR. For instance, using a Ni-B catalyst immersed in a 1 M KOH containing 0.3 M ethanol, it was observed that the EOR peak current density increases (from 1.5 to 7.5 mA cm^{-2}) with an increase in temperature (from 10 to 35 °C).⁸⁷ Higher temperatures allow overcoming the energy activation barrier, which is defined as the minimal energy that should be achieved for an electrochemical reaction to occur. In the case of the electrooxidation of small organic molecules, the activation barrier depends on the catalytic properties of the anode, the potential applied on the electrode/electrolyte interface, the reaction pathway, the rate limiting step, and the relative surface coverage of adsorbed intermediates and products on the catalyst surface.⁸⁸ The relationship between the activation energy (E_a) and the temperature (T) is given by the Arrhenius equation⁸⁹ as seen in eqn (19),

$$k = Ae^{-\frac{E_a}{RT}} \quad (19)$$

where k is the reaction rate constant, A is the frequency factor that measures the rate at which collisions occur, and R is the universal gas constant. The Arrhenius equation predicts a decrease in the E_a when temperature rises. When a reaction is occurring, an increase in the temperature leads to a lower interfacial charge-transfer resistance, and faster kinetics are then observed.⁹⁰ In electrochemical experimentation, the apparent activation energy of a half-reaction at a given potential, denoted as $E_{a(\text{app})}$, is related to the E_a at zero overpotential according to eqn (20),⁸⁹

$$E_{a(\text{app})} = E_a - \beta\eta \quad (20)$$

where β is a coefficient that depends on the experimental conditions. The $E_{a(\text{app})}$ can be obtained by plotting the measured current *versus* the temperature using the Arrhenius model (eqn (21)).⁹¹

$$E_{a(\text{app})} = -2.303R \left[\frac{d \log j}{d(1/T)} \right] \quad (21)$$

The $E_{a(\text{app})}$ is useful for assessing the electrooxidation activity of a catalyst surface. This parameter has been determined, for instance, on a Ni/C electrocatalysts for the GOR by varying the temperature from 2 to 40 °C. The calculated $E_{a(\text{app})}$ was 20.4 kJ mol⁻¹.⁸⁴ Meanwhile, polycrystalline Ni foil was evaluated as a catalyst for the EOR in the temperature range from 15 to 25 °C, resulting in a calculated $E_{a(\text{app})}$ of 49 kJ mol⁻¹.⁹² Using Cu as a catalyst, the MOR was conducted in the temperature range from 30 to 69 °C in 0.1 M NaOH solutions, resulting in a $E_{a(\text{app})}$ value of 33.5 kJ mol⁻¹.⁷⁹

- *Mass transport and conductivity:* with the increase of temperature, the diffusion coefficient of the alcohol molecules in the electrolyte solution increases,^{93,94} enhancing the mass transfer of the alcohol from the bulk solution to the electrode surface. This was observed, for example, for ethanol molecules diffusing from the bulk of the electrolyte to the surface of a polycrystalline Ni foil investigated in the temperature range from -15 to 10 °C.⁹⁵ Additionally, higher temperatures lead to increased transfer of charged species. The specific conductivity of KOH, which is used as a primary supporting electrolyte in industrial alkaline electrolyzers, increases with the temperature, as reported previously for the concentration interval from 0.1 to 48 wt% KOH.⁷⁴ In commercial electrolyzers, elevated temperatures (80–90 °C) are used, which also ensures a lower electrolyte resistance.^{27,96}

- *Stability:* a crucial requirement for industrial alkaline electrolyzers is the selection of electrode materials that are not only active, but also long-term stable. The electrode systems should be designed for low-maintenance, lifetimes of at least five years, and with a minimal loss of performance over time as energy consumption represent a large portion of hydrogen production cost.⁹⁷ However, achieving long-term



stability is challenging due to the highly corrosive conditions of alkaline electrolyzers (elevated temperatures and highly alkaline electrolytes). Recently, there has been a focus on stainless steels and nickel alloys as anode materials for water electrolysis, which can exhibit good corrosion resistance under such operating conditions,⁹⁸ while other catalysts may not be sufficiently stable under the same conditions. For instance, it has been demonstrated that porous cobalt suffers a fast degradation at *ca.* 90 °C in 30–40 wt% KOH solutions; however, with the addition of nickel, the material becomes more stable.⁸⁶ Investigation in terms of stability is not limited to the catalysts, but also other cell components, such as the electrolyte and membrane. For instance, an electrolyzer comprising a polymer electrolyte, namely, quaternary ammonia poly(*N*-methyl-piperidine-*co*-*p*-terphenyl), which possesses high ionic conductivity and chemical stability, could operate at *ca.* 80 °C for a period of 100 h with a high power density.⁹⁹ While it is essential to study stability under such operating temperatures to assess the applicability of HWE, there are only limited studies that report the AOR at elevated temperatures. Recently, Ghosh and colleagues performed stability tests describing the effect of elevated temperature on the stability of the Ni mesh-supported Ni₃N catalyst during the benzyl alcohol oxidation reaction. The stability of the electrode was quantified as the variation of the current density over 30 min electrolysis, a decrease of the current density was observed, however, this was explained by the depletion of benzyl alcohol over time.²⁷ Additional relevant examples can be found in reports covering the AOR driven by catalysts containing noble metals. For instance, White and colleagues performed the GOR on PdNi/Ni at 80 °C. Chronoamperometric tests performed at 0.865 V *vs.* RHE showed a decrease in current density by roughly 50% over a period of 2 h.¹⁰⁰ However, it is unclear if the decrease in current density is due to the depletion of glycerol or to stability issues.

Temperature is thus an important parameter that has a strong influence on several aspects of an electrolysis process. Investigating the efficiency of anode materials at elevated temperatures is essential to develop sufficiently active and long-term stable electrocatalysts for industrial applications. In CWE, elevated temperatures (80–90 °C) are typically employed. Since the boiling point of the solution is shifted to higher temperatures with an increase in KOH concentrations, an alkaline electrolyzer could even be operated at temperatures substantially higher than 100 °C when KOH concentrations are within 80–85 wt%.¹⁰¹ Yet, optimal operating temperature range for the AOR is currently unknown, and the amount of literature on electrocatalysts at different elevated operating temperatures is limited. The scarce number of studies available really show an opportunity for the HWE community to more rigorously evaluate the stability of AOR catalysts at elevated temperatures accompanied by sufficient control experiments to adequately assess the catalytic properties and

electrochemical stability of the anodes, as well as other important performance indicators which will be discussed in detail in section 3.

In summary, this section provided an overview of the AOR tested under the conditions relevant for industrial water electrolysis in alkaline media. Table 2 shows a list of electrocatalysts evaluated towards various alcohol oxidation reactions under such conditions, namely, elevated temperatures, high current densities or concentrated electrolytes. It is important to highlight that, to the best of our knowledge, only one report describes electrocatalyst performance under these three relevant conditions simultaneously.²⁷ Investigations such as this one are urgently needed to facilitate the assessment of electrocatalyst applicability and, thereby, to further advance the HWE field.

3 Additional targets for HWE

One of the most promising aspects of exploring alternative anode reactions for water electrolysis is the possibility of converting low-cost organic compounds, such as bio-based alcohols, into value-added products, while concomitantly producing hydrogen. Hence, in contrast to CWE, where the only by-product is oxygen, HWE requires additional considerations specific to the anode reaction. As discussed earlier, possible products of the electrooxidation of alcohols in alkaline media are aldehydes/ketones, carboxylates and carbonate. The composition of the product mixture depends on the catalyst and alcohol used, and on the electrolysis conditions under which the reaction proceeds.¹¹² Because of this, there are specific targets required for HWE, additional to those discussed in the previous section for CWE. These targets consider, firstly, the selectivity of the reaction, and secondly, the fate of the product (or the mixture of products) obtained from the AOR. In the following section, these two are discussed in detail.

3.1 High selectivity

In the context of catalysis, the International Union of Pure and Applied Chemistry (IUPAC) defines selectivity as the ratio of products obtained from given reactants.¹¹³ For electrocatalytic reactions, selectivity is often expressed in terms of Faradaic efficiency (FE), which is defined as the number of moles of product obtained relative to the amount that could have been produced if all the total charge passed during the reaction would have been used to generate that product, according to Faraday's electrolysis laws.^{114,115} A FE of 1 (or 100% if expressed as percentage) indicates the absence of competing electrochemical reactions. In the case of HWE, FEs near 100% are desirable to maximize the yield of the target product while minimizing the formation of undesired products. However, recent literature indicates that achieving high yields and high selectivity towards a single valuable product is challenging due to the substantial activity-selectivity trade-off exhibited by reported electrocatalytic materials based on earth-abundant



Table 2 Reported electrocatalytic materials based on non-noble metals for the alcohol oxidation reaction evaluated under industrially relevant conditions for alkaline water electrolysis (high current density, high electrolyte concentration, and/or elevated temperature)

Electrocatalyst	Electrolyte	Alcohol	Performance ^a	Temperature (°C)	Ref.
Cu bars	0.1 M NaOH	0.2 M methanol	0.884 V@0.35 mA, 30 °C 0.719 V@0.35 mA, 40 °C 0.699 V@0.35 mA, 50 °C 0.683 V@0.35 mA, 60 °C 0.668 V@0.35 mA, 70 °C	30–70	79
Ni/graphene porous-3D	1 M KOH	0.2–2 M methanol	1.58 V@43.09 mA cm ⁻² in 0.2 M methanol 1.58 V@51.55 mA cm ⁻² in 0.5 M methanol 1.58 V@63.09 mA cm ⁻² in 0.75 M methanol 1.58 V@66.76 mA cm ⁻² in 1 M methanol 1.58 V@74.64 mA cm ⁻² in 2 M methanol	RT	81
Ni/NiO/rGO	3 M KOH	2 M methanol	1.6 V@400 mA cm ⁻²	RT	102
Ni/NiO/RG-400	1 M KOH	1 M methanol	1.607 V@79.5 mA cm ⁻²	RT	
Ni _{0.6} Zn _{0.4}	1 M KOH	0.1 M methanol	1.557 V@10 mA cm ⁻²	RT	103
NiCu/C	1 M KOH	1 M methanol	1.55 V@41.1 mA cm ⁻²	RT	104
Ni ₃ B-NF	6 M KOH	0.5 M methanol	1.53 V@62 A g ⁻¹	RT	77
Ni/PDPA-FTO	0.1 M KOH	1 M methanol	1.55 V@0.039 mA cm ⁻²	RT	80
Ni ₃ Co/CNT	1 M NaOH	1 M methanol or ethanol	1.796 V@213 mA cm ⁻² in methanol 1.796 V@181 mA cm ⁻² in ethanol	RT	54
NiO _x /MWCNTs-O _x	1 M KOH	0.5 M methanol, ethanol or glycerol	1.48 V@0.1 mA in methanol 1.46 V@0.1 mA in ethanol 1.38 V@0.1 mA in glycerol	RT	17
Nickel foil	0.1 M NaOH	0.5 M ethanol	1.55 V@10 mA cm ⁻² , 15 °C 1.48 V@10 mA cm ⁻² , 25 °C	-5–25	92
MnO ₂ –NiO/MWCNTs	1 M KOH	0.1 M methanol or ethanol	1.53 V@0.05 mA cm ⁻² in methanol 1.56 V@0.05 mA cm ⁻² in ethanol	35–55	83
Ni/graphite	1 M NaOH	0.1 M methanol, ethanol, 1-propanol or 2-propanol	1.54 V@6.75 mA cm ⁻² in 1-propanol 1.54 V@16.35 mA cm ⁻² in 2-propanol 1.54 V@18.68 mA cm ⁻² in ethanol 1.54 V@21.66 mA cm ⁻² in methanol	RT	47
NiO	1 M KOH	0.05 M ethanol or ethylene glycol	1.49 V@7.5 mA cm ⁻² in ethanol 1.467 V@7.5 mA cm ⁻² in ethylene glycol	RT	49
Cu ₈₀ Co ₂₀ hydroxycarbonate	1 M KOH	0.1 M ethanol, ethylene glycol, or glycerol	1.6 V@7.85 mA cm ⁻² in ethanol 1.6 V@23.36 mA cm ⁻² in ethylene glycol 1.6 V@40.37 mA cm ⁻² in glycerol	RT	105
CoBi@rGO	1 M KOH	1 M ethanol	1.687 V@10.25 mA cm ⁻²	RT	106
Cu-doped NiOOH	1 M KOH	1 M ethanol	1.72 V@227 mA cm ⁻²	RT	45
M-PHNs (M = CoNi, Co, Ni)	1 M KOH	1 M ethanol	1.39 V@10 mA cm ⁻² with M=CoNi 1.53 V@10 mA cm ⁻² with M=Co 1.55 V@10 mA cm ⁻² with M=Ni	RT	107
Co ₃ O ₄	5 M KOH	0.5–1.5 M C3-alcohols	1.296 V@10 mA cm ⁻² in 0.5 M glycerol 1.343 V@10 mA cm ⁻² in 0.75 M 1,2-propanediol	RT	108



Table 2 (continued)

Electrocatalyst	Electrolyte	Alcohol	Performance ^a	Temperature (°C)	Ref.
Ni(OH) ₂	2 M LiOH, NaOH, KOH or CsOH	0.1 M glycerol	1.388 V@10 mA cm ⁻² in 0.75 M 1,3-propanediol 1.422 V@10 mA cm ⁻² in 1.5 M 2-propanol 1.436 V@10 mA cm ⁻² in 1.5 M 1-propanol 1.6 V@58.0 mA cm ⁻² in NaOH 1.6 V@59.2 mA cm ⁻² in LiOH 1.6 V@64.6 mA cm ⁻² in CsOH 1.6 V@76.1 mA cm ⁻² in KOH	RT	58
NF	0.5 M KOH	0.1 M isopropanol	1.5 V@33.0 mA, 25 °C 1.5 V@36.9 mA, 30 °C 1.5 V@49.2 mA, 40 °C 1.5 V@56.2 mA, 50 °C 1.5 V@60.5 mA, 60 °C 1.5 V@63.0 mA, 70 °C	25–70	85
Ni/C	0.1 M NaOH	0.1 M glycerol	1.6 V@19.52 mA g _{metal} ⁻¹ , 2 °C 1.6 V@22.85 mA g _{metal} ⁻¹ , 5 °C 1.6 V@25.41 mA g _{metal} ⁻¹ , 10 °C 1.6 V@35.20 mA g _{metal} ⁻¹ , 20 °C 1.6 V@41.87 mA g _{metal} ⁻¹ , 40 °C	2–40	84
NiOx/MWCNTs-ox	1 or 7 M KOH	1 M glycerol	1.314 V@10 mA cm ⁻² in 1 M KOH 1.276 V@10 mA cm ⁻² in 7 M KOH	RT	48
Ni ₃ N/NM Ni(OH) ₂	6 M KOH 1, 2 or 5 M KOH	0.1 M benzyl alcohol 8 M benzyl alcohol	1.45 V@0.538 A cm ⁻² 1.45 V@24.2 mA cm ⁻² in 1 M KOH 1.45 V@36.7 mA cm ⁻² in 2 M KOH 1.45 V@66.5 mA cm ⁻² in 5 M KOH	85 RT	27 75
Au/CoOOH Mn-doped NiS Ni _x B CoOOH	1 M KOH 1 M KOH 1 M KOH 1 M KOH	0.1 M benzyl alcohol 0.1 M HMF 0.01 M HMF 0.01 M HMF	1.3 V@340 mA cm ⁻² 1.3 V@50 mA cm ⁻² 1.45 V@100 mA cm ⁻² 1.2 V@20 mA cm ⁻²	RT RT RT RT	109 64 110 111

Abbreviations: RT: room temperature; rGO: reduced graphene oxide; RG: 3d porous graphene network; NF: nickel foam; PDPA-FTO: polydiphenylamine-fluorine doped tin oxide; CNT: carbon nanotubes; MWCNTs-O_x: oxygen-functionalized multiwalled carbon nanotubes; MWCNTs: multiwalled carbon nanotubes; PHN: perforated hydroxide nanosheets; NM: nickel mesh. ^a All potentials are indicated in the RHE scale.

materials.¹³ Namely, high selectivities are typically observed at relatively low electrode potentials. As a consequence, the current density is also relatively low, which translates into a low hydrogen production rate in a hybrid water electrolyzer. This trade-off is visualized in Fig. 4, being more pronounced for polyhydric alcohols (such as glycerol) than for monoalcohols. Hence, a selectivity target towards a certain product with simultaneous hydrogen production should be techno-economically justified,¹⁹ taking into account market requirements for the specific, targeted AOR product. Such requirements include not only the rate of production but also the product specifications (e.g., purity), which, in turn,

depends on its application. Yet, since HWE is an emerging technology, feasible selectivity targets are currently unknown. Nonetheless, it is clear that a high selectivity is desirable. In this section, we focus on identifying reports concerning the electrochemical conversion of alcohols with FEs above 90% achieved with non-noble metal-based electrocatalysts, and identify conditions under which high selectivities have been achieved.

Starting with the electrooxidation of polyhydric alcohols, particularly diols and triols such as ethylene glycol and glycerol, respectively, the highest FEs have been reported for formate production on Ni-based catalysts. Morales *et al.*



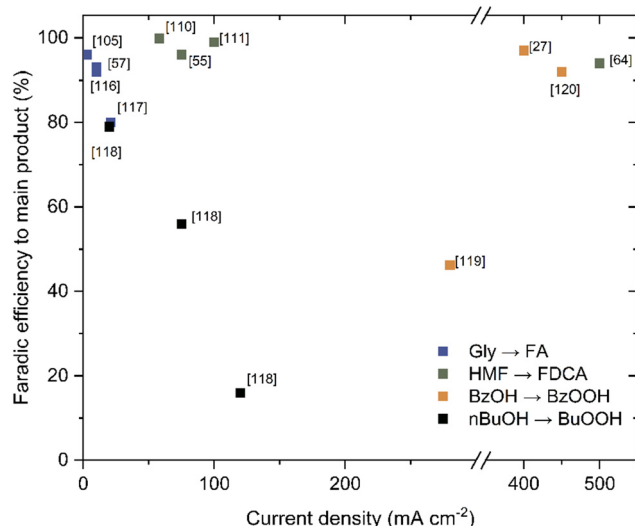


Fig. 4 Faradaic efficiencies and associated current densities for various alcohol oxidation catalyzed by electrocatalysts based on earth-abundant materials.^{27,55,57,64,105,110,111,116–120} Abbreviations: Gly: glycerol; FA: formic acid; HMF: hydroxymethylfurfural; FDCA: 2,5-furandicarboxylic acid; BzOH: benzyl alcohol; BzOOH: benzoic acid; *n*-BuOH: 1-butanol; BuOOH: butanoic acid.

reported electrolysis of glycerol using MWCNTs-supported Ni oxide nanoparticles as electrocatalyst.⁴⁸ Using a recirculating flow-through cell and 1 M KOH electrolyte solution containing initially 100 mM glycerol, a FE of nearly 96% was achieved after 1 h electrolysis at a low constant potential of 1.31 V *vs.* RHE. Yet, lower FEs were observed at longer electrolysis times at the same potential, with a value of 67% after 24 h. The decrease in FE over time was attributed to an increase in the rate of the competing formate oxidation reaction (with carbonate as product) as the concentration of glycerol decreased. The FE also decreased when electrolysis was conducted at higher electrode potentials (1.41 and 1.51 V *vs.* RHE), alongside a substantial increase in current density. Furthermore, in this study a vast shift in product selectivity was seen depending on the concentration of supporting electrolyte (KOH) that was used. With an electrolyte concentration of 7 M, the formation of oxalate was favored, while high selectivity towards formate was observed in 1 M KOH. In a report by Chen and coworkers, electrolysis of 50 mM ethylene glycol was conducted in 1 M KOH solution using NiO nanosheets as electrocatalyst.⁴⁹ Authors found a selectivity (defined as the moles of product relative to the moles of ethylene glycol consumed during the reaction) of 95% towards formate when electrolysis was conducted at 1.5 V *vs.* RHE. High FEs towards formate have also been reported with Ni-containing bimetallic systems during the GOR. For instance, Ni-foam supported NiCo₂O₄ achieved an average FE of about 95% during 48 h electrolysis at 1.4 V *vs.* RHE refreshing the electrolyte (0.1 M glycerol in 1 M KOH solution) every 12 h.⁶⁰ Notably, the current densities measured during this experiment varied between 100 and 250 mA cm⁻², and exhibited a stable performance in the

electrolysis periods from 12 to 48 h. Another example is found in the report by Li and coworkers,⁶³ where the performance of carbon cloth-supported Ni–Mo nitride nanoplates was investigated for the GOR. By conducting electrolysis for 12 h at 1.35 V *vs.* RHE in 1 M KOH electrolyte (containing initially 100 mM glycerol), FEs between 94 and 98% towards formate were achieved.

Selectivity can be heavily influenced not only by the concentration of the supporting electrolyte, as discussed above for the MWCNTs-supported Ni oxide,⁴⁸ but also by the chemical nature of the supporting electrolyte. As an example, in a study conducted on the GOR catalyzed by Ni(OH)₂, it was found that cation selection influenced the selectivity of the reaction towards formate as the main product, with FE values in the order CsOH < KOH < NaOH < LiOH. Authors proposed that Li cations stabilized the aldehyde intermediates, preventing their further oxidation, and leaned towards C–C cleavage to form formate.⁵⁸ Further evidence can be found in another study on the GOR using CuO as a catalyst.⁷⁰ It was found that changing the nature of the electrolyte, and consequently the pH of the solution from 13 (0.1 M NaOH) to 7 (0.1 M Na₂B₄O₇), a significant increase in the selectivity towards dihydroxyacetone, a high-value product, was observed. These examples show that besides careful catalyst selection, a toolbox for selectivity steering can also be found in the selection of electrolyte composition. This also reiterates the importance of testing the catalytic systems at elevated electrolyte concentrations as discussed in the section 2.3.

It is important to note that obtaining GOR products of higher value than formate, such as dihydroxyacetone, tartronate, mesoxalate or lactate, with a relatively high selectivity (>50%) has mainly been reported with catalysts containing precious metals including Au and Pt.^{121–124} A similar situation is observed for the partial electrooxidation of benzyl alcohol (BOR) which can yield benzaldehyde and benzoate.¹²⁵ High selectivities (and relatively high FEs) towards the formation of benzaldehyde have been reported for Au-based catalysts,¹²⁶ particularly under mildly alkaline environments and relatively low electrode potentials.¹⁰⁹ Meanwhile, Ni-based electrocatalysts are reported to favor the formation of benzoate as the main organic product in a broad range of operating conditions.⁴³ Under typical lab-scale conditions (1 M KOH, room temperature), FEs of nearly 100% towards benzoate were reported during the BOR using Ni nanoparticles supported on N-doped carbon as electrocatalyst. In a recent work by Ghosh *et al.*,²⁷ a remarkable 97% FE towards the same product was achieved using Ni mesh-supported Ni₃N under industry-like conditions for alkaline water electrolysis (6 M KOH solution at 85 °C). Likely, a fast conversion of benzyl alcohol to benzaldehyde is followed by the further oxidation of this product, which is favored by Ni.¹²⁷ In this context, strategies have been proposed to prevent the overoxidation of benzaldehyde. For instance, Xu *et al.* reported selectivities of nearly 100% towards benzaldehyde, using NiO as electrocatalyst, which

was achieved by tuning the alkalinity and concentration of cations (K^+ , Na^+ , Li^+) thereby inhibiting the oxidation of benzaldehyde.¹²⁸ Yet, it is important to note that the reported selectivities were calculated as moles of target product relative to the sum of detected products (and not with respect to the moles of reactant), and achieving FEs higher than 90% required a careful optimization of the electrolyte composition and of the applied currents. Another interesting approach was proposed by Shi and coworkers,⁷⁵ who developed a three-phase (organic liquid, inorganic liquid and solid) system consisting of super-organophobic Ni(OH)_2 nanosheets supported on super-organophilic carbon, located at an organic–water boundary. The system achieved FEs of up to 97% towards benzaldehyde and current densities of about 180 mA cm^{-2} . Both of these approaches could be further explored and potentially applied to prevent the overoxidation of other organic molecules, hence boosting the selectivity towards a wide variety of target products.

2,5-Furandicarboxylic acid (FDCA) is an important organic chemical in the context of green chemistry with potential applications in the polymers industry.¹²⁹ It can be obtained from the electrooxidation of 5-(hydroxymethyl)furfural (HMF) or 2,5-bis(hydroxymethyl)furan (BHMF) with FEs of about 95% using Co-based electrocatalytic materials. For instance, Zhang and coworkers used cobalt carbonate hydroxide nanoarrays as electrocatalyst. The CoOOH sites, formed under electrolysis conditions, exhibited a FE of 99% for the conversion of HMF to FDCA during electrolysis at 1.42 V vs. RHE in 1 M KOH.¹¹¹ Liu *et al.* reported a mild corrosion treatment of Co foam, which resulted in a FE of 95% towards FDCA when used as a catalyst for BHMF oxidation at 1.4 V vs. RHE in 1 M KOH solution.⁵⁹ Conducting the same treatment of Co foam in the presence of NiSO_4 resulted in the introduction of Ni in the electrocatalyst, which in turn increased the FE and yield of FDCA measured under the same conditions. Other bimetallic systems, including NiCo ,^{55,130} NiFe ^{131,132} and MnNi ⁶⁴ have also been reported to possess a high selectivity towards the same product (FEs > 90%). However, it is important to note that the performance of materials towards the electrooxidation of alcohols is not only influenced by metal composition, but also by other factors including crystallinity and phase composition, particle size and particle distribution, surface area and porosity, as well as the choice of supporting materials, binders, among others.^{17,51,133} Achieving highly selective conversions requires therefore careful engineering of the electrochemical interfaces, involving both electrolyte and electrode, in addition to a careful selection of electrolysis conditions and reactor engineering.^{128,134}

3.2 Circularity

Selectivity is a decisive factor for the (industrial) applicability of HWE technologies. Limited selectivity leads to the formation of complex mixtures, the separation of which is

energy- and cost-intensive. In cases in which selectivity (section 3.1) is insufficient and product separation (section 4.1) is not techno-economically feasible, the result is the formation of a waste stream. In the case of the AOR in alkaline media, such stream typically consists of a mixture of carboxylates, aldehydes and/or ketones, as well as the unreacted alcohol and carbonate. Therefore, it is important to identify possible routes for circularity, taking into account the fate of the product mixture. In this section, a brief overview of potential uses for the product mixtures generated by the AOR is provided, which could, in the future, add value to the electrolysis process as a whole.

Organic acid-containing streams can find use in bioelectrochemical systems (BES). For instance, in a bioreactor, electroactive bacteria can metabolize organic acids and transfer the extracted electrons across their cell membrane to a current collector. Thus, while uptaking the organic acid, they are able to aid in the removal of the organic acid. This system can be coupled with an anaerobic membrane bioreactor, an emerging wastewater treatment technology, increasing the energy-efficiency of this process.¹³⁵ Another example of BES are the anaerobic digestion reactors: complex waste mixtures can be fed to microorganisms to produce a gaseous combination of methane and carbon dioxide (*i.e.* biogas) that can be used as a feedstock for a variety of processes.¹³⁶ Thus, BES represent a potential route for the utilization of HWE byproduct streams.

A possible route to upgrade HWE byproducts is Kolbe electrolysis, in which carboxylic acids can be transformed into longer-chain alkanes or alkenes.¹³⁷ The dimerization of carboxylic acids into longer-chain alkenes can additionally facilitate product recovery since the resulting mixtures could spontaneously separate into different phases.¹³⁸ Although during this process CO_2 is produced, as shown in Fig. 5, this stream can be captured and potentially fed to CO_2 electrolyzers to generate commercially interesting chemicals such as formic acid, methane, ethylene and methanol, representing another source of value. Kolbe electrolysis has been applied to upgrade fermentation streams which consist of mixtures of organic acids. A study conducted on the Kolbe electrolysis of organic acid-containing wastewater originating from corn beer fermentation showed that a liquid “drop-in” fuel was produced, which could be utilized without the need for downstream processing.¹³⁸ Furthermore, Rosa and coworkers showed recently that, using Kolbe electrolysis, hexanoic acid could be transformed into 1-decane with FEs up to 68%, and it was argued that the obtained fuel and its properties are akin to aviation fuel and could therefore be a possible substitution for kerosene.¹³⁹ Finally, Neubert and



Fig. 5 A general reaction scheme for Kolbe electrolysis.



colleagues showed that from 12.4 mol of a mixture of carboxylic acids originating from a microbial conversion, a 1 L of fuel could be produced through Kolbe electrolysis. This was done for less than one euro in energy costs, achieving a FE of 70%.¹⁴⁰ Remarkably, the FE for the Kolbe electrolysis of organic acid mixtures was high compared to those using a single carboxylic acid, which is ideal for mixtures originated from microbial processes or from hybrid water electrolyzers, which convert waste alcohols into a complex mixture of carboxylic acids.

Considering the number of processes that can be powered by renewable electricity, a circular dependency can be pictured for the aforementioned process as illustrated in Fig. 6. The field of HWE could benefit greatly from the exploration of such routes to generate additional value from HWE byproducts.

4 Enhancing the applicability of HWE

Reactor design has a substantial impact on the efficiency of any electrolysis process. However, lab-scale research innovations in the field of electrocatalysis, and particularly in the field of HWE, are mainly leaned towards the discovery of new catalytic materials rather than optimization of the electrochemical cell. Rational design of electrolysis reactors can lead to the enhancement of mass transfer, the decrease in ohmic resistances¹⁴¹ and, in some instances, has been

shown to be able to steer selectivity.¹²⁶ In fact, leaps in the performance of water electrolysis can also be made in the area of reactor design, as demonstrated by the novel capillary-fed electrolysis (CFE) cell introduced by Hodges and coworkers in 2022.¹⁴² Employing commercial catalysts, a significant increase in energy-efficiency was achieved mainly due the CFE's ability to reduce the mass transport limitations associated with a two-phase flow and gas bubble formation which block the catalytic sites. A schematic description of this configuration is shown in Fig. 7a. In this section, we will discuss strategies related to reactor design that show promise in the context of the AOR. In addition to this, we also discuss in this section process design, particularly in relation to the separation of organic products from the electrolyte. An overview of process approaches which could potentially be explored in the context of HWE are presented, highlighting three main goals: achieving cost-efficient product separation, steering reaction selectivity, and reducing ohmic and mass transfer limitations.

4.1 Product separation

As discussed previously, the field of HWE faces a variety of challenges related to the implementation of the electrooxidation of organic compounds as alternative anode reactions. One of the challenges is related to the formation of complex mixtures of organic products resulting from the

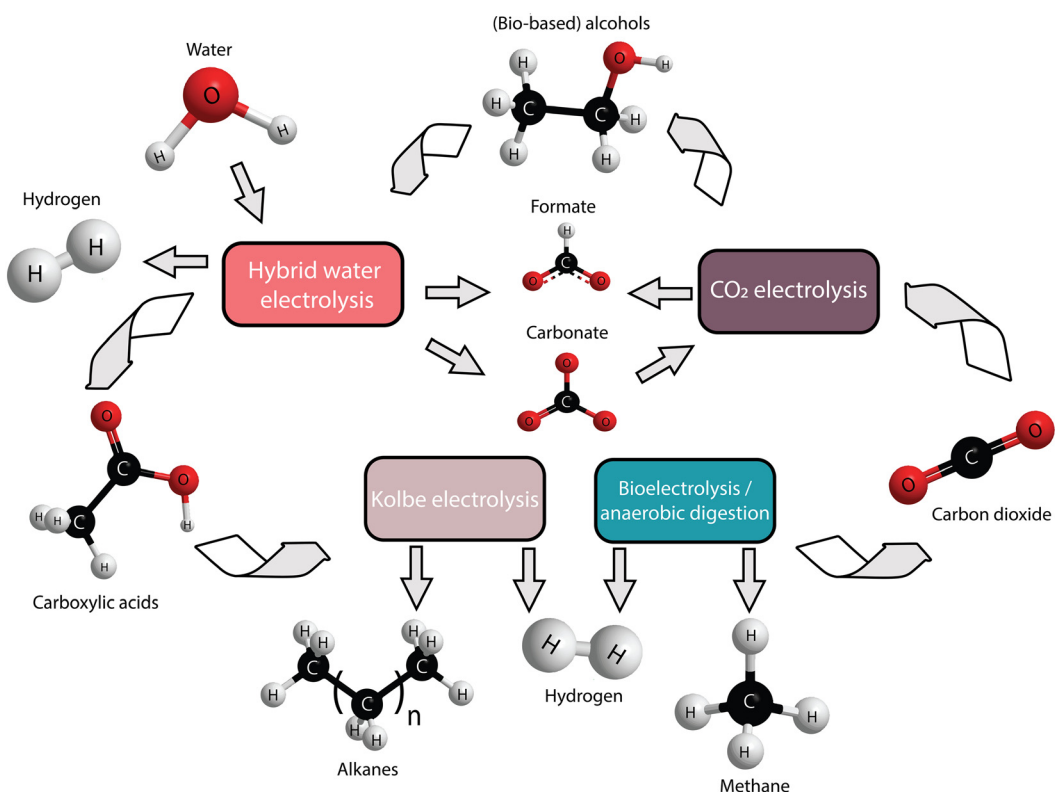


Fig. 6 An illustration of possible circular dependencies between electrolysis reactions powered by renewable energy, and their associated reactants and products.

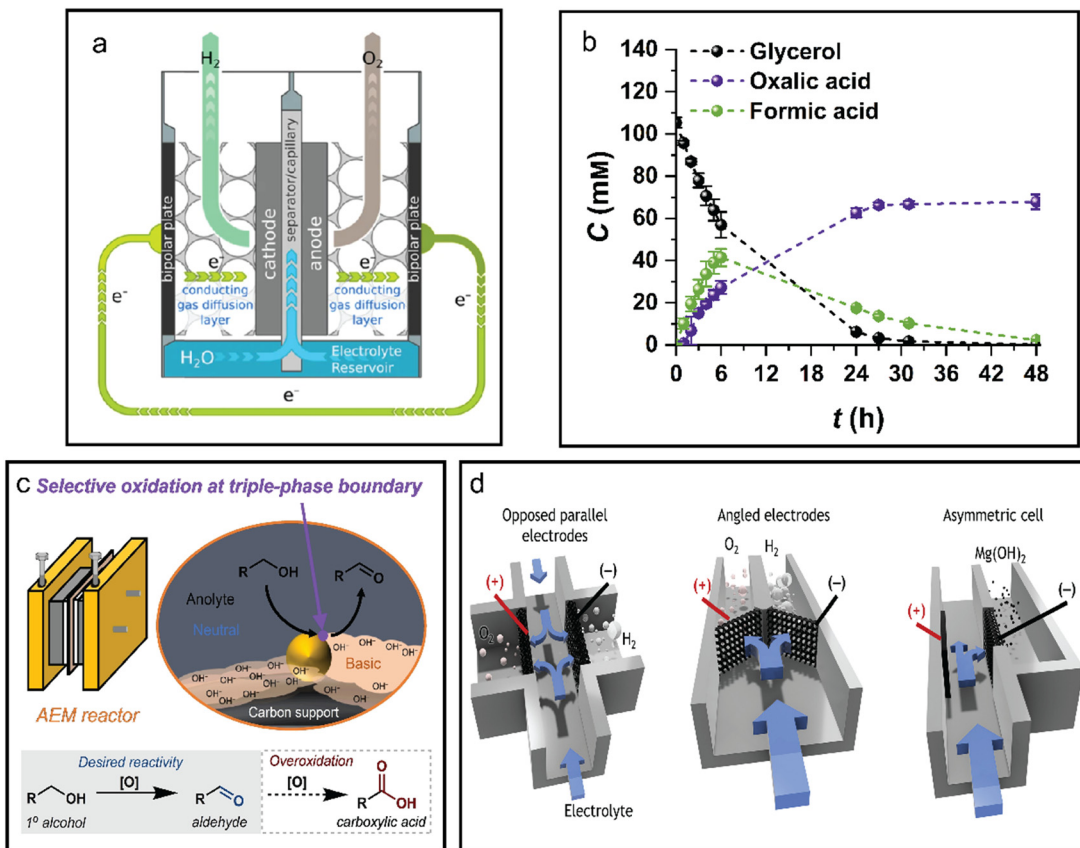


Fig. 7 (a) A graphical depiction of a capillary-fed water electrolyzer. Adapted from ref. 142 under a CC BY 4.0 license; (b) the product distribution of prolonged glycerol electrolysis on multiwalled carbon nanotube-supported Ni oxide at industrially relevant electrolyte concentration (7 M KOH) and its effect on product selectivity. Reprinted with permission from ref. 48 copyright 2024 American Chemical Society; (c) an example of the effect of a tailored triple phase boundary on the selectivity of an AOR. Reprinted with permission from ref. 126 copyright 2024 John Wiley & Sons, Inc; (d) an example of membraneless electrolyzer configurations for CWE. Reprinted from ref. 141 copyright 2024, with permission from Elsevier.

electrooxidation process, which require separation from the electrolyte and purification. As pointed out by various techno-economic analyses (TEAs) conducted on HWE, separation costs are likely to become an important part of upscaling costs and, hence, a deciding factor for industrial viability.^{19,143} Thus, giving early thought to the selection of separation processes required to isolate HWE products already at lab-scale is essential to identify suitable methods and enable industrial adoption.

The partial electrooxidation of an alcohol in alkaline environments yields two types of products, namely, the aldehyde/ketone or the carboxylate anion, which often have a very high affinity for aqueous solutions.¹⁴⁴ The difficulty in separating the product from the solution is further increased by the relatively low concentrations at which these products are obtained. A parallel can be made with the bioconversion of renewables through fermentation, which has shown to effectively and sustainably produce carboxylic acids,¹⁴⁵ but suffer from separation issues from the fermentation broth.¹⁴⁴ Approaches for effective separation in the field of bioconversion mainly involve the use of ion-exchange and resin adsorption to transfer the carboxylic acids into solutions which could be distilled or crystallized for product

recovery.¹⁴⁵ However these methods are still marked by their energy intensiveness, low yields, and sometimes could cause product degradation, as is the case for distillation due to its relatively high temperature requirements.¹⁴⁶ More novel approaches can be found in the use of ionic liquids to extract carboxylic acids from aqueous solutions.¹⁴⁴ In particular, reactive extraction has gained traction as an emerging technology for this purpose. In reactive extraction, the organic acids form complexes with so-called “extractants.” These complexes have a high affinity for an organic phase and simplify the separation.¹⁴⁷ For example, through reactive extraction and the use of ionic liquids, glycolic acid, a value-added product obtained from the GOR, was separated from an aqueous phase with *ca.* 99% efficiency.¹⁴⁸ Reactive extraction could also be a possible route for scalable separation, as the extractant can be recovered and reused. In this case, the main challenge is identifying and/or developing case-specific, environmentally-friendly extractants.¹⁴⁹

Another separation approach is electrodialysis, which shows high potential due to its ability to separate organic products with high affinity for the aqueous phase.¹⁵⁰ An additional advantage is that, integrating electrodialysis into the existing electrolyzer-energy recovery network is more

straightforward than other approaches, and it does not require the use of hazardous solvents. This has already been shown for the separation of lactic acid from a beet molasses feed stream, recovering the carboxylic acid with a purity of 95%.¹⁵¹ Another example was reported by Wang and coworkers, who showed that a product stream, originating from the electroreduction of CO₂, could be separated into a 3.5 M formic acid, KOH-containing aqueous solution from the initial electrolyte (KHCO₃) at a current efficiency of 50%.¹⁵² Furthermore, the authors highlighted that the KOH obtained as byproduct could be reused to uptake CO₂ for further electroreduction, demonstrating that these processes can be further integrated.

A final, relatively unexplored approach to facilitate separation is electrochemical purification. This is particularly promising for cases in which a wide product distribution is obtained from the electrolysis of an alcohol, as is often observed for polyhydric alcohols such as glycerol. During the GOR, glycerol is consumed and eventually depleted. Without glycerol competing for the oxidation sites on the surface of the catalyst, the GOR products can be further oxidized. At prolonged electrolysis times, only the compounds that are electrochemically stable under the employed electrolysis conditions will remain in the solution. An example of this can be seen in a study in which the GOR was conducted with MWCNTs-supported Ni oxide nanoparticles as electrocatalysts. After 6 h of electrolysis at 1.5 V vs. RHE in 7 M KOH solution using a recirculating flow-through reactor, a mixture of at least eight different carboxylates was found, among which formate and oxalate were the major products in a concentration ratio of about 4:3. As electrolysis progressed for an additional 42 h, only two products remained, oxalate and acetate, in a concentration ratio of 60:1, whereas all other GOR products were fully oxidized to carbonate. The evolution of the major products is shown in Fig. 7b.⁴⁸ Scaling this approach up could involve the electrochemical “aging” of processed electrolyte batches, all while still producing hydrogen at the cathode, and thereby obtaining an organic product with increased purity. It should be noted that in this approach the target organic product is still in the aqueous phase, which means that further separation is still required, but it would significantly reduce the complexity of the preceding separation process.

There is a scarce amount of literature incorporating any of the previously mentioned separation techniques in tandem with HWE. With this section, we hope to highlight some possible future research directions addressing the additional challenge of product separation in HWE.

4.2 Steering selectivity

The added benefit of oxidizing an organic compound in HWE is twofold: a decrease in energy requirements to produce hydrogen, and the generation of value-added compounds at the anode. However, obtaining concurrently a high current density (which translates in a high hydrogen

production rate) and a selective reaction (to produce a valuable compound with low separation costs) has proven difficult.¹³ Thus, the design of highly selective electrode/electrolyte interfaces operating at high current densities is still needed to advance the HWE field. However, less attention has been given to a complementary route: developing suitable reactor designs. It is known from the field of heterogeneous catalysis that reactor design can influence substantially the selectivity of a catalytic process.^{153,154} In electrocatalysis, there are examples of the relation between reactor design and product selectivity. For instance, in the context of the electroreduction of CO₂, membrane electrode assembly (MEA)-type reactors often yield higher selectivities towards C₂⁺ products, as opposed to H-type cells due to the increased surface engineering that is possible at the catalyst/membrane interface. H-cells additionally suffer from low current densities due to the large diffusion layer size at the electrode/electrolyte interface.¹⁵⁵ In a report by Gabardo and coworkers, specific anion exchange membrane (AEM) placement in a MEA-type reactor allowed for the generation of a high local pH, thus favoring C–C coupling, and thereby increasing the selectivity for the targeted (C²⁺) products compared to other tested reactor configurations, namely, two flow cells tested at neutral and high pH values, this can be seen as an example of successful surface engineering.¹⁵⁶ Another approach was shown by Han and coworkers, who compared two different types of gas flows over a gas diffusion electrode (GDE), referred to as “flow-by” and “flow-through.” Compared to the former, the “flow-through” approach resulted in a significant increase in selectivity of the CO₂ conversion to ethylene under otherwise identical conditions.¹⁵⁷

In the case of HWE, and particularly of the AOR, literature reports on novel reactor designs that boost the reaction selectivity, involving for instance tuning reactor size or type, is rather sparse. However, the reports available show that the reactor can have a significant influence in the AOR selectivity. For example, using a microfluidic cell design tailored for the GOR resulted in an increase in deep oxidation products, that is, compounds which are near or at their final possible oxidation state, compared to a typical lab-scale three-electrode configuration cell. This was explained by the increase of sequential oxidation reactions that occur, possibly induced by differences in mass transfer between the two types of reactors.¹⁵⁸ One of the most remarkable examples was reported in 2021 by Ido and colleagues, who investigated the electrooxidation of benzoic acid in 1 M KOH solution.¹²⁶ This primary alcohol was oxidized to its aldehyde with 100% selectivity in an AEM configuration, an increase of 47% compared to a three-electrode electrolysis batch cell. In the batch setup, the decreased selectivity was attributed to the further oxidation of the benzaldehyde to benzoate. In the AEM configuration, overoxidation was prevented by forming a triple-phase boundary between the catalyst particles, the anolyte and the ionomer used.¹²⁶ This approach, depicted in Fig. 7c, remains relatively unexplored in the field of HWE.



Overall, these results show that, even when using the same catalyst and electrolyte, selectivity can be altered by tailoring the reactor design, representing a promising route for the further advancement of HWE.

4.3 Addressing ohmic resistance and mass transfer limitations

In addition to enabling possibilities to steer selectivity, reactor design can also help to decrease ohmic resistances, increasing thereby the efficiency of both the anodic and cathodic electrocatalytic processes. For CWE, a 200 year long reactor evolution has been targeting these limitations.¹⁴² The cell efficiency, especially at high current densities, has shown to be influenced strongly by the ohmic resistance presented in the cell.¹⁵⁹ Thus, novel cell architecture designs are often proposed with the goal of minimizing ohmic resistance. An example of this is the so-called “zero-gap” electrolyzer.¹⁵⁹ However, an important component of industrial electrolyzers are the separators (membranes or diaphragms) which are essential since they maintain the purity of the products and prevent the formation of explosive hydrogen/oxygen mixtures. These component impose substantial ohmic resistances, tend to be quite expensive and have been known to limit the life-time of an electrolyzer.¹⁴¹ In the context of HWE, if the AOR takes place at sufficiently low overpotentials, it is possible that the OER does not take place, and thus, explosive hydrogen/oxygen mixtures would not be formed. This could imply that a hybrid water electrolyzer could operate without the need of a separator as long as the products are sufficiently stable and/or fast removed. Early research concerning membraneless electrolyzers (MEs), examples of which can be found in Fig. 7d, has shown good promise for CWE.¹⁴¹ In such designs, using fluid dynamics, the electrolyte flow forces the separation of the two gas products and thereby forgoes the need for a membrane. This approach could be integrated with an increased simplicity for HWE in comparison to CWE. Nevertheless, product crossover is an important aspect to consider. While crossover is often quantified in reports dealing with direct alcohol fuel cells,¹⁶⁰ this topic is frequently neglected in the field of HWE. Product crossover can reduce the energy efficiency and product yield, for instance, by oxidizing the produced hydrogen at the anode or reducing the organic products at the cathode. Thus, it is undesired, and preventing it requires developing suitable membranes and/or tailored MEs designs.

In addition to the membrane, electrodes may exhibit limitations in mass transfer due to obstruction of their channel and pores, causing an increased ohmic resistance. In particular, precipitation of carbonates could reduce the lifespan of electrolyzer components and increase maintenance costs.^{161,162} As an alternative, solid-state anion-exchange membranes (AEM) have been extensively used in alkaline electrolyzers to replace liquid electrolytes. This technology can solve some of the aforementioned problems since they do not present precipitation from carbonates due to lack of metallic cations. Additionally, the gas permeability

is smaller, avoiding gas crossover. Mass transfer can also become a limiting factor during an electrolysis process, particularly at industrially relevant current densities.⁷¹ It has an increased importance in HWE as the concentration of the organic additive, *e.g.*, the alcohol, is often much lower than that of the electrolyte. In this context, studies on the effect of mass transfer and enhancement thereof through reactor design is an unexplored opportunity in the field of HWE. Increasing the mass transfer through reactor design, to the benefit of reactor performance, is more thoroughly studied for the AOR in the field of alcohol fuel cells. An example can be found in a study conducted on direct methanol fuel cells, where El-Zoheiry and colleagues proposed new flow field designs to optimize the methanol distribution over a catalytically active surface, increasing drastically the power density of the device.¹⁶³ Finally, rational reactor design can also be optimized by the use of theoretical modelling,¹⁶⁴ as has been done in the fields of CWE and fuel cells.^{163,165}

5 Conclusion and outlook

Hybrid water electrolysis (HWE) is a young field that aims to achieve hydrogen production at low energy costs with simultaneous generation of a value-added product. Meanwhile, the more established field of conventional water electrolysis (CWE) is directing its efforts towards performance targets for industrial implementation. Such direction is missing in the HWE field, as clear targets remain unavailable. This review has emphasized the recent progress in the testing of HWE systems involving the alcohol electrooxidation reaction (AOR) under conditions relevant to industrial alkaline water electrolysis, in particular regarding overpotential, current density, electrolyte composition and operating temperature. An overview of the state of the art was showcased for these different parameters. Besides these targets, HWE faces other challenges: first, the need for a highly selective anodic reaction, which often comes at the cost of a limitation in current density, and by extension, in the rate of hydrogen production. A selective anodic reaction is essential to increase the techno-economic benefit extracted from HWE, not only by increasing the amount of product generated, but also to simplify downstream separation. In general, HWE research can benefit from extensive techno-economic analyses to justify research into a particular feedstock. The selection of the feedstock should consider not only its theoretical electrooxidation potential but also other factors such as their availability, toxicity and the effectiveness of their conversion into valuable products with a high selectivity and low energy costs. Comparing the scales of both feedstock's availability and market demand of target products (including hydrogen) can also provide valuable information. Furthermore, for cases where high selectivity cannot be achieved, we discussed possible circularity routes which could avert the need for expensive separation processes. Second, tailored reactor and process design are needed for further advancement of HWE technologies. We presented examples from the literature showing that tailored reactor designs can



increase the selectivity of an electrolysis process and/or increase the efficiency by reducing ohmic resistances. Furthermore, we identified process design choices and novel techniques that could aid in the separation of the complex product mixtures streamed from HWE processes. Taking into account the high potential HWE has to address certain shortcomings of CWE, we now provide concrete recommendations that we hope will facilitate the industrial application of this technology:

1) Testing novel catalytic materials under industrially relevant conditions is essential to assess their applicability. While such conditions are largely unknown for HWE, it is evident that high current densities are desirable, as they translate in product yields. However, there is a limited number of literature reports where novel electrocatalysts are evaluated under current densities above 0.1 A cm^{-2} . Increasing the prevalence of such tests in the literature will provide valuable information for comparison with industrial CWE and will facilitate the assessment of their potential applicability. We thus propose that future research should target current densities higher than 0.1 A cm^{-2} , preferably moving up into the ampere level, with a focus not only on the required electrode potentials, but also on selectivity and long-term electrochemical stability. Conducting such measurements in concentrated electrolytes, and elevated temperatures and pressures will be essential to elucidate to which extent HWE technologies can be implemented in existing CWE devices. Moreover, while technically challenging, *in situ* and *operando* investigations of the AOR in concentrated electrolytes, at elevated temperatures and/or at relevant current densities are urgently needed to increase the understanding of the electrochemical systems under these conditions, which is also essential to provide fair comparison with state-of-the-art, industrial alkaline water electrolysis. In addition to this, current literature lacks in-depth understanding of the competition between the AOR and the OER under industrially relevant conditions. Thus, it is recommended that investigations on novel AOR electrocatalysts are complemented with oxygen monitoring techniques such as DEMS, gas chromatography or rotating ring disk electrode voltammetry, to further aid in the design of highly selective alcohol conversion processes towards valuable products.

2) Clearly defining and accurately determining selectivity parameters should become standard protocol in HWE electrocatalytic research. As the field steadily diverges from OER studies, where selectivity aspects are often not emphasized, the HWE field deals with complex product mixtures and selectivity plays a crucial role in evaluating the applicability of this technology. The lack of standard reporting practices in the field of HWE is problematic, especially when early TEAs indicate that product separation could become the largest cost factor for industrial application of HWE. An electrocatalyst with a high selectivity could circumvent this problem. Consequently, selectivity should be regarded as a central performance metric in electrocatalyst

evaluation and therefore should be reported rigorously in HWE research. Lastly, product quantification should be extended to also incorporate species found in the cathodic compartment, to aid in the quantification of membrane crossover and increase completeness of selectivity measurements.

3) Increasing research efforts on tailored design of HWE reactors and processes, addressing challenges that cannot be fixed solely by the electrocatalyst. Interdisciplinary research for novel reactor design, aided by theoretical modelling, can prove of great importance to boost the applicability of HWE, as it has done so for CWE. Furthermore, the field still requires identification of specific processes in which HWE could provide additional merit for near-future applications, for example in bio electrochemical systems.

While literature and research concerning HWE has been growing rapidly in the past years, there is still vast potential for progress, particularly concerning the eventual step from the academic space to industrial application. We hope that with this review, the included literature and the recommendations provided, the HWE field can find guidance towards further advancement.

Data availability

No primary research results, software or code have been included and no new data were generated or analyzed as part of this review.

Conflicts of interest

The authors declare no conflict of interest.

Acknowledgements

Eleazar Castañeda-Morales is grateful to CONACYT-Mexico for the financial support during his doctoral studies.

References

- 1 A. M. Oliveira, R. R. Beswick and Y. Yan, A green hydrogen economy for a renewable energy society, *Curr. Opin. Chem. Eng.*, 2021, 33, 100701.
- 2 E. Taibi, H. Blanco, R. Miranda and M. Carmo, *Green hydrogen cost reduction: Scaling up electrolyzers to meet the 1.5C climate goal*, International Renewable Energy Agency, Abu Dhabi, 2020, https://www.irena.org/-/media/Files/IRENA/Agency/Publication/%202020/Dec/IRENA_Green_hydrogen_cost_2020.pdf.
- 3 J. Zhu, D. Ciolca, L. Liu, A. Parastaei, N. Kosinov and E. J. M. Hensen, Flame synthesis of Cu/ZnO-CeO₂ catalysts: synergistic metal-support interactions promote CH₃OH selectivity in CO₂ hydrogenation, *ACS Catal.*, 2021, 11, 4880–4892.
- 4 W. Meng, B. C. A. de Jong, H. van de Bovenkamp, G.-J. Boer, G. Leendert Bezemer, A. Iulian Dugulan and J. Xie, Selectivity control between reverse water-gas shift and



Fischer-Tropsch synthesis in carbon-supported iron-based catalysts for CO₂ hydrogenation, *Chem. Eng. J.*, 2024, **489**, 151166.

5 United Nations, *Transforming our world: the 2030 agenda for sustainable development* | Department of Economic and Social Affairs, New York, USA, 2015, <https://sdgs.un.org/sites/default/files/publications/21252030%20Agenda%20for%20Sustainable%20Development%20web.pdf>.

6 A. Ajanovic, M. Sayer and R. Haas, The economics and the environmental benignity of different colors of hydrogen, *Int. J. Hydrogen Energy*, 2022, **47**, 24136–24154.

7 A. Ursua, L. M. Gandia and P. Sanchis, Hydrogen production from water electrolysis: Current status and future trends, *Proc. IEEE*, 2012, **100**, 410–426.

8 R. Soltani, M. A. Rosen and I. Dincer, Assessment of CO₂ capture options from various points in steam methane reforming for hydrogen production, *Int. J. Hydrogen Energy*, 2014, **39**, 20266–20275.

9 N. Thissen, J. Hoffmann, S. Tigges, D. A. M. Vogel, J. J. Thoede, S. Khan, N. Schmitt, S. Heumann, B. J. M. Etzold and A. K. Mechler, Industrially relevant conditions in lab-scale analysis for alkaline water electrolysis, *ChemElectroChem*, 2024, **11**, e202300432.

10 Clean Hydrogen Partnership, *Clean hydrogen joint undertaking: Strategic research and innovation agenda 2021–2027*, 2022, <https://www.clean-hydrogen.europa.eu/system/files/2022-02/Clean%20Hydrogen%20JU%20SRIA%20-20%20approved%20by%20GB%20-%20clean%20for%20publication%20%28ID%2013246486%29.pdf>.

11 X. Xie, L. Du, L. Yan, S. Park, Y. Qiu, J. Sokolowski, W. Wang and Y. Shao, Oxygen evolution reaction in alkaline environment: Material challenges and solutions, *Adv. Funct. Mater.*, 2022, **32**, 2110036.

12 K. Veeramani, G. Janani, J. Kim, S. Surendran, J. Lim, S. C. Jesudass, S. Mahadik, H. Lee, T.-H. Kim, J. K. Kim and U. Sim, Hydrogen and value-added products yield from hybrid water electrolysis: A critical review on recent developments, *Renewable Sustainable Energy Rev.*, 2023, **177**, 113227.

13 F. van Lieshout and D. M. Morales, Anodic reactions in alkaline hybrid water electrolyzers: Activity versus selectivity, *ChemPlusChem*, 2024, **89**, e202400182.

14 S. Anantharaj, S. R. Ede, K. Sakthikumar, K. Karthick, S. Mishra and S. Kundu, Recent trends and perspectives in electrochemical water splitting with an emphasis on sulfide, selenide, and phosphide catalysts of Fe, Co, and Ni: A review, *ACS Catal.*, 2016, **6**, 8069–8097.

15 B. Kumari, M. Braun, S. Cychy, I. Sanjuán, G. Behrendt, M. Behrens, M. Muhler and C. Andronescu, Electrooxidation of the glycerol derivative solketal over Cu–Co hydroxycarbonates to enable the synthesis of glyceric acid, *ChemElectroChem*, 2023, **10**, e202300018.

16 M. K. Goetz, M. T. Bender and K.-S. Choi, Predictive control of selective secondary alcohol oxidation of glycerol on NiOOH, *Nat. Commun.*, 2022, **13**, 5848.

17 E. C. Morales, M. A. Kazakova, A. G. Selyutin, G. V. Golubtsov, D. M. Morales and A. M. Robledo, Competition between the oxygen evolution reaction and the electrooxidation of alcohols on heteroatom-functionalized multi-walled carbon nanotubes-supported Ni oxide catalysts, *Surf. Interfaces*, 2024, **46**, 104026.

18 H. van't Noordeinde and R. Bollen, *Safety aspects of green hydrogen production on industrial scale*, Hydrohub Innovation Program, The Netherlands, 2023, https://www.h2-mobile.fr/uploads/doc_20231114192000.pdf.

19 M. Braun, C. S. Santana, A. C. Garcia and C. Andronescu, From waste to value – Glycerol electrooxidation for energy conversion and chemical production, *Curr. Opin. Green Sustainable Chem.*, 2023, **41**, 100829.

20 M. R. Monteiro, C. L. Kugelmeier, R. S. Pinheiro, M. O. Batalha and A. da Silva César, Glycerol from biodiesel production: Technological paths for sustainability, *Renewable Sustainable Energy Rev.*, 2018, **88**, 109–122.

21 M. Rastogi and S. Shrivastava, Recent advances in second generation bioethanol production: An insight to pretreatment, saccharification and fermentation processes, *Renewable Sustainable Energy Rev.*, 2017, **80**, 330–340.

22 X. Xu, Y. Zhong, M. Wajrak, T. Bhatelia, S. P. Jiang and Z. Shao, Grain boundary engineering: An emerging pathway toward efficient electrocatalysis, *InfoMat*, 2024, **6**, e12608.

23 H. Sun, X. Xu, L. Fei, W. Zhou and Z. Shao, Electrochemical oxidation of small molecules for energy-saving hydrogen production, *Adv. Energy Mater.*, 2024, **14**, 2401242.

24 W. R. Leow, S. Völker, R. Meys, J. E. Huang, S. A. Jaffer, A. Bardow and E. H. Sargent, Electrified hydrocarbon-to-oxygenates coupled to hydrogen evolution for efficient greenhouse gas mitigation, *Nat. Commun.*, 2023, **14**, 1954.

25 S. Watzele, Y. Liang and A. S. Bandarenka, Intrinsic activity of some oxygen and hydrogen evolution reaction electrocatalysts under industrially relevant conditions, *ACS Appl. Energy Mater.*, 2018, **1**, 4196–4202.

26 J. Hu, T. Guo, X. Zhong, J. Li, Y. Mei, C. Zhang, Y. Feng, M. Sun, L. Meng, Z. Wang, B. Huang, L. Zhang and Z. Wang, In situ reconstruction of high-entropy heterostructure catalysts for stable oxygen evolution electrocatalysis under industrial conditions, *Adv. Mater.*, 2024, **36**, 2310918.

27 S. Ghosh, J. N. Hausmann, L. Reith, G. Vijaykumar, J. Schmidt, K. Laun, S. Berendts, I. Zebger, M. Driess and P. W. Menezes, Nitridated nickel mesh as industrial water and alcohol oxidation catalyst: Reconstruction and iron-incorporation matters, *Adv. Energy Mater.*, 2024, **14**, 2400356.

28 Y. M. Hao, H. Nakajima, A. Inada, K. Sasaki and K. Ito, Overpotentials and reaction mechanism in electrochemical hydrogen pumps, *Electrochim. Acta*, 2019, **301**, 274–283.

29 J. Wang, F. Xu, H. Jin, Y. Chen and Y. Wang, Non-noble metal-based carbon composites in hydrogen evolution reaction: Fundamentals to applications, *Adv. Mater.*, 2017, **29**, 1605838.

30 Y. Xu and B. Zhang, Recent advances in electrochemical hydrogen production from water assisted by alternative oxidation reactions, *ChemElectroChem*, 2019, **6**, 3214–3226.



31 C. C. L. McCrory, S. Jung, J. C. Peters and T. F. Jaramillo, Benchmarking heterogeneous electrocatalysts for the oxygen evolution reaction, *J. Am. Chem. Soc.*, 2013, **135**, 16977–16987.

32 W. Zhang, M. Liu, X. Gu, Y. Shi, Z. Deng and N. Cai, Water electrolysis toward elevated temperature: Advances, challenges and frontiers, *Chem. Rev.*, 2023, **123**, 7119–7192.

33 E. López-Fernández, C. Gómez-Sacedón, J. Gil-Rostra, J. P. Espinós, A. R. González-Elipe, F. Yubero and A. de Lucas Consuegra, Nanostructured nickel based electrocatalysts for hybrid ethanol-water anion exchange membrane electrolysis, *J. Environ. Chem. Eng.*, 2022, **10**, 107994.

34 H. Dau, C. Limberg, T. Reier, M. Risch, S. Roggan and P. Strasser, The mechanism of water oxidation: from electrolysis via homogeneous to biological catalysis, *ChemCatChem*, 2010, **2**, 724–761.

35 X. Ren, Y. Zhai, N. Yang, B. Wang and S. Liu, Lattice oxygen redox mechanisms in the alkaline oxygen evolution reaction, *Adv. Funct. Mater.*, 2024, **34**, 2401610.

36 S. Hou, R. M. Kluge, R. W. Haid, E. L. Gubanova, S. A. Watzele, A. S. Bandarenka and B. Garlyyev, A review on experimental identification of active sites in model bifunctional electrocatalytic systems for oxygen reduction and evolution reactions, *ChemElectroChem*, 2021, **8**, 3433–3456.

37 L. Yaqoob, T. Noor and N. Iqbal, Recent progress in development of efficient electrocatalyst for methanol oxidation reaction in direct methanol fuel cell, *Int. J. Energy Res.*, 2021, **45**, 6550–6583.

38 M. Braun and C. Andronescu, Deciphering the electrochemical activity and selectivity of earth-abundant transition metal-based catalysts for the alcohol electrooxidation—Current status, *ChemCatChem*, 2025, **17**, e202402013.

39 S. Möller, S. Barwe, J. Masa, D. Wintrich, S. Seisel, H. Baltruschat and W. Schuhmann, Online monitoring of electrochemical carbon corrosion in alkaline electrolytes by differential electrochemical mass spectrometry, *Angew. Chem., Int. Ed.*, 2020, **59**, 1585–1589.

40 M. Ramdin, O. A. Moults, L. J. P. van den Broeke, P. Gonugunta, P. Taheri and T. J. H. Vlugt, Carbonation in low-temperature CO_2 electrolyzers: Causes, consequences, and solutions, *Ind. Eng. Chem. Res.*, 2023, **62**, 6843–6864.

41 R. Sharifian, R. M. Wagterveld, I. A. Digdaya, C. Xiang and D. A. Vermaas, Electrochemical carbon dioxide capture to close the carbon cycle, *Energy Environ. Sci.*, 2021, **14**, 781–814.

42 X. Zhang, J. Wang, K. Zong, Z. Chen, X. Yang, L. Yang, X. Wang and Z. Chen, Recent advances in non-noble metal-based electrocatalysts for hybrid water electrolysis systems, *Carbon Energy*, 2025, **7**, e679.

43 M. Fleischmann, K. Korinek and D. Pletcher, The oxidation of organic compounds at a nickel anode in alkaline solution, *J. Electroanal. Chem. Interfacial Electrochem.*, 1971, **31**, 39–49.

44 A. Seghiouer, J. Chevalet, A. Barhou and F. Lantelme, Electrochemical oxidation of nickel in alkaline solutions: a voltammetric study and modelling, *J. Electroanal. Chem.*, 1998, **442**, 113–123.

45 H. Wang, A. Guan, J. Zhang, Y. Mi, S. Li, T. Yuan, C. Jing, L. Zhang, L. Zhang and G. Zheng, Copper-doped nickel oxyhydroxide for efficient electrocatalytic ethanol oxidation, *Chin. J. Catal.*, 2022, **43**, 1478–1484.

46 L. M. Reid, T. Li, Y. Cao and C. P. Berlinguet, Organic chemistry at anodes and photoanodes, *Sustainable Energy Fuels*, 2018, **2**, 1905–1927.

47 M. Jafarian, A. Mirzapoor, I. Danaee, S. A. A. Shahnazi and F. Gobal, A comparative study of the electrooxidation of C1 to C3 aliphatic alcohols on Ni modified graphite electrode, *Sci. China:Chem.*, 2012, **55**, 1819–1824.

48 D. M. Morales, D. Jambrec, M. A. Kazakova, M. Braun, N. Sikdar, A. Koul, A. C. Brix, S. Seisel, C. Andronescu and W. Schuhmann, Electrocatalytic conversion of glycerol to oxalate on Ni oxide nanoparticles-modified oxidized multiwalled carbon nanotubes, *ACS Catal.*, 2022, **12**, 982–992.

49 W. Chen, J. Shi, C. Xie, W. Zhou, L. Xu, Y. Li, Y. Wu, B. Wu, Y.-C. Huang, B. Zhou, M. Yang, J. Liu, C.-L. Dong, T. Wang, Y. Zou and S. Wang, Unraveling the electrophilic oxygen-mediated mechanism for alcohol electrooxidation on NiO, *Natl. Sci. Rev.*, 2023, **10**, nwad099.

50 W. Chen, J. Shi, Y. Wu, Y. Jiang, Y.-C. Huang, W. Zhou, J. Liu, C.-L. Dong, Y. Zou and S. Wang, Vacancy-induced catalytic mechanism for alcohol electrooxidation on nickel-based electrocatalyst, *Angew. Chem., Int. Ed.*, 2024, **63**, e202316449.

51 A. C. Brix, M. Dreyer, A. Koul, M. Krebs, A. Rabe, U. Hagemann, S. Varhade, C. Andronescu, M. Behrens, W. Schuhmann and D. M. Morales, Structure-performance relationship of $\text{LaFe}_{1-x}\text{CoO}_3$ electrocatalysts for oxygen evolution, isopropanol oxidation, and glycerol oxidation, *ChemElectroChem*, 2022, **9**, e202200092.

52 M. Nacef, M. L. Chelaghmia, O. Khelifi, M. Pontié, M. Djelaibia, R. Guerfa, V. Bertagna, C. Vautrin-Ul, A. Fares and A. M. Affoune, Electrodeposited Ni on pencil graphite electrode for glycerol electrooxidation in alkaline media, *Int. J. Hydrogen Energy*, 2021, **46**, 37670–37678.

53 B. Habibi and N. Delnavaz, Electrooxidation of glycerol on nickel and nickel alloy (Ni–Cu and Ni–Co) nanoparticles in alkaline media, *RSC Adv.*, 2016, **6**, 31797–31806.

54 Z. Deng, Q. Yi, Y. Zhang and H. Nie, NiCo/C-N/CNT composite catalysts for electro-catalytic oxidation of methanol and ethanol, *J. Electroanal. Chem.*, 2017, **803**, 95–103.

55 Y. Sun, J. Wang, Y. Qi, W. Li and C. Wang, Efficient electrooxidation of 5-hydroxymethylfurfural using Co-doped Ni_3S_2 catalyst: Promising for H_2 production under industrial-level current density, *Adv. Sci.*, 2022, **9**, 2200957.

56 B. Zhu, B. Dong, F. Wang, Q. Yang, Y. He, C. Zhang, P. Jin and L. Feng, Unraveling a bifunctional mechanism for



methanol-to-formate electro-oxidation on nickel-based hydroxides, *Nat. Commun.*, 2023, **14**, 1686.

57 X. Yu, R. B. Araujo, Z. Qiu, E. C. dos Santos, A. Anil, A. Cornell, L. G. M. Pettersson and M. Johnsson, Hydrogen evolution linked to selective oxidation of glycerol over CoMoO₄—A theoretically predicted catalyst, *Adv. Energy Mater.*, 2022, **12**, 2103750.

58 J. Wu, J. Li, Y. Li, X.-Y. Ma, W.-Y. Zhang, Y. Hao, W.-B. Cai, Z.-P. Liu and M. Gong, Steering the glycerol electro-reforming selectivity via cation–intermediate interactions, *Angew. Chem., Int. Ed.*, 2022, **61**, e202113362.

59 J. Liu, B. Zhu, Y. Zhong, S. Fan, L. Huai, H. Hu, Y. Yang, J. Zhang and C. Chen, Turning damages into benefits: Corrosion-engineered cobalt foam for highly efficient biomass upgrading coupled with H₂ generation, *Chem. Eng. J.*, 2023, **472**, 144877.

60 W. Luo, H. Tian, Q. Li, G. Meng, Z. Chang, C. Chen, R. Shen, X. Yu, L. Zhu, F. Kong, X. Cui and J. Shi, Controllable electron distribution reconstruction of spinel NiCo₂O₄ boosting glycerol oxidation at elevated current density, *Adv. Funct. Mater.*, 2024, **34**, 2306995.

61 Z. He, J. Hwang, Z. Gong, M. Zhou, N. Zhang, X. Kang, J. W. Han and Y. Chen, Promoting biomass electrooxidation via modulating proton and oxygen anion deintercalation in hydroxide, *Nat. Commun.*, 2022, **13**, 3777.

62 Q. Wang, X. Zhou, H. Jin, L. Guo, Y. Wu and S. Ren, Cu-doped Ni₃S₂ electrocatalyst for glycerol oxidation coupling to promote hydrogen evolution reaction, *Fuel*, 2024, **377**, 132770.

63 Y. Li, X. Wei, L. Chen, J. Shi and M. He, Nickel-molybdenum nitride nanoplate electrocatalysts for concurrent electrolytic hydrogen and formate productions, *Nat. Commun.*, 2019, **10**, 5335.

64 S. Li, S. Wang, Y. Wang, J. He, K. Li, Y. Xu, M. Wang, S. Zhao, X. Li, X. Zhong and J. Wang, Doped Mn enhanced NiS electrooxidation performance of hmf into fdca at industrial-level current density, *Adv. Funct. Mater.*, 2023, **33**, 2214488.

65 H. Sun, L. Li, Y. Chen, H. Kim, X. Xu, D. Guan, Z. Hu, L. Zhang, Z. Shao and W. Jung, Boosting ethanol oxidation by NiOOH-CuO nano-heterostructure for energy-saving hydrogen production and biomass upgrading, *Appl. Catal., B*, 2023, **325**, 122388.

66 T. Andreu, M. Mallafré, M. Molera, M. Sarret, R. Oriol and I. Sirés, Effect of thermal treatment on nickel-cobalt electrocatalysts for glycerol oxidation, *ChemElectroChem*, 2022, **9**, e202200100.

67 J. Hao, J. Liu, D. Wu, M. Chen, Y. Liang, Q. Wang, L. Wang, X.-Z. Fu and J.-L. Luo, In situ facile fabrication of Ni(OH)₂ nanosheet arrays for electrocatalytic co-production of formate and hydrogen from methanol in alkaline solution, *Appl. Catal., B*, 2021, **281**, 119510.

68 P. Puthongkham and B. J. Venton, Recent advances in fast-scan cyclic voltammetry, *Analyst*, 2020, **145**, 1087–1102.

69 G. R. Chodankar, M. R. Waikar, S. A. Sawant, N. R. Chodankar, S. D. Dhas, U. V. Shembade, A. R. Sonkawade, A. V. Moholkar and R. G. Sonkawade, Tailoring the electrochemical performance of monoclinic Ni₂P₂O₇ microstructure across different alkaline electrolytes, *Int. J. Hydrogen Energy*, 2024, **60**, 657–667.

70 C. Liu, M. Hirohara, T. Maekawa, R. Chang, T. Hayashi and C.-Y. Chiang, Selective electro-oxidation of glycerol to dihydroxyacetone by a non-precious electrocatalyst – CuO, *Appl. Catal., B*, 2020, **265**, 118543.

71 K. Zeng and D. Zhang, Recent progress in alkaline water electrolysis for hydrogen production and applications, *Prog. Energy Combust. Sci.*, 2010, **36**, 307–326.

72 J. de Paula, D. Nascimento and J. J. Linares, Influence of the anolyte feed conditions on the performance of an alkaline glycerol electroreforming reactor, *J. Appl. Electrochem.*, 2015, **45**, 689–700.

73 F. Sultan, J. Zhu, D. I. Medina, P. P. Pescarmona, J. L. Cholula-Díaz and D. M. Morales, Nickel cobalt oxide-based heterostructures as electrocatalysts for the oxygen evolution reaction at industry-relevant conditions, *Int. J. Hydrogen Energy*, 2025, **114**, 440–451.

74 R. J. Gilliam, J. W. Graydon, D. W. Kirk and S. J. Thorpe, A review of specific conductivities of potassium hydroxide solutions for various concentrations and temperatures, *Int. J. Hydrogen Energy*, 2007, **32**, 359–364.

75 R. Shi, X. Zhang, C. Li, Y. Zhao, R. Li, G. I. N. Waterhouse and T. Zhang, Electrochemical oxidation of concentrated benzyl alcohol to high-purity benzaldehyde via superwetting organic-solid-water interfaces, *Sci. Adv.*, 2024, **10**, eadn0947.

76 K. Malaie, M. R. Ganjali, T. Alizadeh and P. Norouzi, Simple electrochemical preparation of nanoflake-like copper oxide on Cu-plated nickel foam for supercapacitor electrodes with high areal capacitance, *J. Mater. Sci.: Mater. Electron.*, 2017, **28**, 14631–14637.

77 J. Li, F. Luo, Q. Zhao, L. Xiao, J. Yang, W. Liu and D. Xiao, Crystalline nickel boride nanoparticle agglomerates for enhanced electrocatalytic methanol oxidation, *Int. J. Hydrogen Energy*, 2019, **44**, 23074–23080.

78 C. Andronescu, S. Seisel, P. Wilde, S. Barwe, J. Masa, Y.-T. Chen, E. Ventosa and W. Schuhmann, Influence of temperature and electrolyte concentration on the structure and catalytic oxygen evolution activity of nickel–iron layered double hydroxide, *Chem. – Eur. J.*, 2018, **24**, 13773–13777.

79 H. Heli, M. Jafarian, M. G. Mahjani and F. Gobal, Electro-oxidation of methanol on copper in alkaline solution, *Electrochim. Acta*, 2004, **49**, 4999–5006.

80 A. Raveendran, M. Chandran, S. M. Wabaidur, M. A. Islam, R. Dhanusuraman and V. K. Ponnusamy, Facile electrochemical fabrication of nickel-coated polydiphenylamine (Ni/PDPA) nanocomposite material as efficient anode catalyst for direct alcohol fuel cell application, *Fuel*, 2022, **324**, 124424.

81 H. Zhu, J. Wang, X. Liu and X. Zhu, Three-dimensional porous graphene supported Ni nanoparticles with enhanced catalytic performance for methanol



electrooxidation, *Int. J. Hydrogen Energy*, 2017, **42**, 11206–11214.

82 S. Gamil, W. M. A. E. Rouby, M. Antuch and I. T. Zedan, Nano-hybrid layered double hydroxide materials as efficient catalysts for methanol electro-oxidation, *RSC Adv.*, 2019, **9**, 13503–13514.

83 M. Shojaeifar, M. B. Askari, S. R. S. Hashemi and A. D. Bartolomeo, MnO_2 – NiO –MWCNTs nanocomposite as a catalyst for methanol and ethanol electro-oxidation, *J. Phys. D: Appl. Phys.*, 2022, **55**, 355502.

84 V. L. Oliveira, C. Morais, K. Servat, T. W. Napporn, P. Olivi, K. B. Kokoh and G. Tremiliosi-Filho, Kinetic investigations of glycerol oxidation reaction on Ni/C, *Electrocatalysis*, 2015, **6**, 447–454.

85 J. van Drunen, T. W. Napporn, B. Kokoh and G. Jerkiewicz, Electrochemical oxidation of isopropanol using a nickel foam electrode, *J. Electroanal. Chem.*, 2014, **716**, 120–128.

86 F. P. Lohmann-Richters, S. Renz, W. Lehnert, M. Müller and M. Carmo, Review—Challenges and opportunities for increased current density in alkaline electrolysis by increasing the operating temperature, *J. Electrochem. Soc.*, 2021, **168**, 114501.

87 S.-J. Zhang, Y.-X. Zheng, L.-S. Yuan and L.-H. Zhao, Ni–B amorphous alloy nanoparticles modified nanoporous Cu toward ethanol oxidation in alkaline medium, *J. Power Sources*, 2014, **247**, 428–436.

88 C. A. Angelucci, H. Varela, E. Herrero and J. M. Feliu, Activation energies of the electro-oxidation of formic acid on Pt(100), *J. Phys. Chem. C*, 2009, **113**, 18835–18841.

89 J. Masa, S. Barwe, C. Andronescu and W. Schuhmann, On the theory of electrolytic dissociation, the greenhouse effect, and activation energy in (electro)catalysis: A tribute to Svante Augustus Arrhenius, *Chem. – Eur. J.*, 2019, **25**, 158–166.

90 S. Piontek, C. Andronescu, A. Zaichenko, B. Konkena, K. J. Puring, B. Marler, H. Antoni, I. Sinev, M. Muhler, D. Mollenhauer, B. R. Cuenya, W. Schuhmann and U.-P. Apfel, Influence of the Fe:Ni ratio and reaction temperature on the efficiency of $(\text{Fe}_x\text{Ni}_{1-x})_9\text{S}_8$ electrocatalysts applied in the hydrogen evolution reaction, *ACS Catal.*, 2018, **8**, 987–996.

91 L. V. Kumar, S. Addo Ntim, O. Sae-Khow, C. Janardhana, V. Lakshminarayanan and S. Mitra, Electro-catalytic activity of multiwall carbon nanotube–metal (Pt or Pd) nano-hybrid materials synthesized using microwave-induced reactions and their possible use in fuel cells, *Electrochim. Acta*, 2012, **83**, 40–46.

92 A. F. B. Barbosa, V. L. Oliveira, J. van Drunen and G. Tremiliosi-Filho, Ethanol electro-oxidation reaction using a polycrystalline nickel electrode in alkaline media: Temperature influence and reaction mechanism, *J. Electroanal. Chem.*, 2015, **746**, 31–38.

93 S. Pothoczki, L. Pusztai and I. Bakó, Temperature dependent dynamics in water–ethanol liquid mixtures, *J. Mol. Liq.*, 2018, **271**, 571–579.

94 A. Klinov and I. Anashkin, Diffusion in binary aqueous solutions of alcohols by molecular simulation, *Processes*, 2019, **7**, 947.

95 A. Chandrasekar, D. Flynn and E. Syron, Operational challenges for low and high temperature electrolyzers exploiting curtailed wind energy for hydrogen production, *Int. J. Hydrogen Energy*, 2021, **46**, 28900–28911.

96 M. Schalenbach, A. R. Zeradjanin, O. Kasian, S. Cherevko and K. J. J. Mayrhofer, A perspective on low-temperature water electrolysis – Challenges in alkaline and acidic technology, *Int. J. Electrochem. Sci.*, 2018, **13**, 1173–1226.

97 M. David, C. Ocampo-Martínez and R. Sánchez-Peña, Advances in alkaline water electrolyzers: A review, *J. Energy Storage*, 2019, **23**, 392–403.

98 Nickel Institute, *Corrosion resistance of nickel and nickel-containing alloys in caustic soda and other alkalies (CEB-2) – A practical guide to the use of nickel-containing alloys No 281*, 2020.

99 H. Peng, Q. Li, M. Hu, L. Xiao, J. Lu and L. Zhuang, Alkaline polymer electrolyte fuel cells stably working at 80 °C, *J. Power Sources*, 2018, **390**, 165–167.

100 J. White, L. Peters, D. Martín-Yerga, I. Terekhina, A. Anil, H. Lundberg, M. Johnsson, G. Salazar-Alvarez, G. Henriksson and A. Cornell, Glycerol electro-oxidation at industrially relevant current densities using electrodeposited PdNi/Ni-foam catalysts in aerated alkaline media, *J. Electrochem. Soc.*, 2023, **170**, 086504.

101 A. T. Hamada, M. F. Orhan and A. M. Kannan, Alkaline fuel cells: Status and prospects, *Energy Rep.*, 2023, **9**, 6396–6418.

102 K. Zhang, Y. Han, J. Qiu, X. Ding, Y. Deng, Y. Wu, G. Zhang and L. Yan, Interface engineering of Ni/NiO heterostructures with abundant catalytic active sites for enhanced methanol oxidation electrocatalysis, *J. Colloid Interface Sci.*, 2023, **630**, 570–579.

103 S. Wei, L. Qian, D. Jia and Y. Miao, Synthesis of 3D flower-like $\text{Ni}_{0.6}\text{Zn}_{0.4}\text{O}$ microspheres for electrocatalytic oxidation of methanol, *Electrocatalysis*, 2019, **10**, 540–548.

104 Y. An, H. Ijaz, M. Huang, J. Qu and S. Hu, The one-pot synthesis of CuNi nanoparticles with a Ni-rich surface for the electrocatalytic methanol oxidation reaction, *Dalton Trans.*, 2020, **49**, 1646–1651.

105 M. Braun, G. Behrendt, M. L. Krebs, P. Dimitri, P. Kumar, I. Sanjuán, S. Cyhy, A. C. Brix, D. M. Morales, J. Hörlöck, B. Hartke, M. Muhler, W. Schuhmann, M. Behrens and C. Andronescu, Electro-oxidation of alcohols on mixed copper–cobalt hydroxycarbonates in alkaline solution, *ChemElectroChem*, 2022, **9**, e202200267.

106 A. V. Munde, B. B. Mulik, P. P. Chavan, V. S. Sapner, S. S. Narwade, S. M. Mali and B. R. Sathe, Electrocatalytic ethanol oxidation on cobalt–bismuth nanoparticle-decorated reduced graphene oxide (Co–Bi@rGO): Reaction pathway investigation toward direct ethanol fuel cells, *J. Phys. Chem. C*, 2021, **125**, 2345–2356.

107 W. Wang, Y.-B. Zhu, Q. Wen, Y. Wang, J. Xia, C. Li, M.-W. Chen, Y. Liu, H. Li, H.-A. Wu and T. Zhai, Modulation of molecular spatial distribution and chemisorption with



perforated nanosheets for ethanol electro-oxidation, *Adv. Mater.*, 2019, **31**, 1900528.

108 S. Sun, L. Sun, S. Xi, Y. Du, M. U. A. Prathap, Z. Wang, Q. Zhang, A. Fisher and Z. J. Xu, Electrochemical oxidation of C3 saturated alcohols on Co_3O_4 in alkaline, *Electrochim. Acta*, 2017, **228**, 183–194.

109 Z. Li, Y. Yan, S.-M. Xu, H. Zhou, M. Xu, L. Ma, M. Shao, X. Kong, B. Wang, L. Zheng and H. Duan, Alcohols electrooxidation coupled with H_2 production at high current densities promoted by a cooperative catalyst, *Nat. Commun.*, 2022, **13**, 147.

110 S. Barwe, J. Weidner, S. Czychy, D. M. Morales, S. Dieckhöfer, D. Hiltrop, J. Masa, M. Muhler and W. Schuhmann, Electrocatalytic oxidation of 5-(hydroxymethyl) furfural using high-surface-area nickel boride, *Angew. Chem., Int. Ed.*, 2018, **57**, 11460–11464.

111 R. Zhang, S. Jiang, Y. Rao, S. Chen, Q. Yue and Y. Kang, Electrochemical biomass upgrading on CoOOH nanosheets in a hybrid water electrolyzer, *Green Chem.*, 2021, **23**, 2525–2530.

112 Y. Zhao, E. M. Björk, Y. Yan, P. Schaaf and D. Wang, Recent progress in transition metal based catalysts and mechanism analysis for alcohol electrooxidation reactions, *Green Chem.*, 2024, **26**, 4987–5003.

113 T. I. U. of P. and A. Chemistry (IUPAC), IUPAC – selectivity (S05563), <https://goldbook.iupac.org/terms/view/S05563>, (accessed 3 July 2024).

114 P. A. Kempler and A. C. Nielander, Reliable reporting of Faradaic efficiencies for electrocatalysis research, *Nat. Commun.*, 2023, **14**, 1158.

115 T. F. Fuller and J. N. Harb, *Electrochemical Engineering*, John Wiley & Sons, 2018.

116 L. Fan, Y. Ji, G. Wang, J. Chen, K. Chen, X. Liu and Z. Wen, High entropy alloy electrocatalytic electrode toward alkaline glycerol valorization coupling with acidic hydrogen production, *J. Am. Chem. Soc.*, 2022, **144**, 7224–7235.

117 S. Czychy, S. Lechler, Z. Huang, M. Braun, A. C. Brix, P. Blümller, C. Andronescu, F. Schmid, W. Schuhmann and M. Muhler, Optimizing the nickel boride layer thickness in a spectroelectrochemical ATR-FTIR thin-film flow cell applied in glycerol oxidation, *Chin. J. Catal.*, 2021, **42**, 2206–2215.

118 S. E. Michaud, M. M. Barber, K. E. R. Cruz and C. C. L. McCrory, Electrochemical oxidation of primary alcohols using a Co_2NiO_4 catalyst: Effects of alcohol identity and electrochemical bias on product distribution, *ACS Catal.*, 2023, **13**, 515–529.

119 W. Su, X. Zheng, W. Xiong, Y. Ouyang, Z. Zhang, W. Zeng, H. Duan, X. Chen, P. Su, Z. Sun and M. Yuan, Open Active Sites in Ni-Based MOF with High Oxidation States for Electrooxidation of Benzyl Alcohol, *Inorg. Chem.*, 2024, **63**, 12572–12581.

120 H. Huang, C. Yu, X. Han, H. Huang, Q. Wei, W. Guo, Z. Wang and J. Qiu, Ni, Co hydroxide triggers electrocatalytic production of high-purity benzoic acid over 400 mA cm⁻², *Energy Environ. Sci.*, 2020, **13**, 4990–4999.

121 Z. Zhang, L. Xin, J. Qi, D. J. Chadderdon, K. Sun, K. M. Warsko and W. Li, Selective electro-oxidation of glycerol to tartronate or mesoxalate on Au nanoparticle catalyst via electrode potential tuning in anion-exchange membrane electro-catalytic flow reactor, *Appl. Catal., B*, 2014, **147**, 871–878.

122 C. Dai, L. Sun, H. Liao, B. Khezri, R. D. Webster, A. C. Fisher and Z. J. Xu, Electrochemical production of lactic acid from glycerol oxidation catalyzed by AuPt nanoparticles, *J. Catal.*, 2017, **356**, 14–21.

123 Y. Zhou, Y. Shen, X. Luo, G. Liu and Y. Cao, Boosting activity and selectivity of glycerol oxidation over platinum–palladium–silver electrocatalysts via surface engineering, *Nanoscale Adv.*, 2020, **2**, 3423–3430.

124 W.-Y. Zhang, X.-Y. Ma, S.-Z. Zou and W.-B. Cai, Recent advances in glycerol electrooxidation on Pt and Pd: from reaction mechanisms to catalytic, *J. Electrochem.*, 2021, **27**, 233–256.

125 E. A. Mayeda, L. L. Miller and J. F. Wolf, Electrooxidation of benzylic ethers, esters, alcohols, and phenyl epoxides, *J. Am. Chem. Soc.*, 1972, **94**, 6812–6816.

126 Y. Ido, A. Fukazawa, Y. Furutani, Y. Sato, N. Shida and M. Atobe, Triple-phase boundary in anion-exchange membrane reactor enables selective electrosynthesis of aldehyde from primary alcohol, *ChemSusChem*, 2021, **14**, 5405–5409.

127 A. J. Motheo, G. Tremiliosi-Filho, E. R. Gonzalez, K. B. Kokoh, J.-M. Léger and C. Lamy, Electrooxidation of benzyl alcohol and benzaldehyde on a nickel oxy-hydroxide electrode in a filter-press type cell, *J. Appl. Electrochem.*, 2006, **36**, 1035–1041.

128 L. Xu, Z. Huang, M. Yang, J. Wu, W. Chen, Y. Wu, Y. Pan, Y. Lu, Y. Zou and S. Wang, Salting-out aldehyde from the electrooxidation of alcohols with 100% selectivity, *Angew. Chem., Int. Ed.*, 2022, **61**, e202210123.

129 V. Ashokkumar, R. Venkatkarthick, S. Jayashree, S. Chuetor, S. Dharmaraj, G. Kumar, W.-H. Chen and C. Ngamcharussrivichai, Recent advances in lignocellulosic biomass for biofuels and value-added bioproducts – A critical review, *Bioresour. Technol.*, 2022, **344**, 126195.

130 X. Deng, M. Li, Y. Fan, L. Wang, X.-Z. Fu and J.-L. Luo, Constructing multifunctional ‘nanoplatelet-on-nanoarray’ electrocatalyst with unprecedented activity towards novel selective organic oxidation reactions to boost hydrogen production, *Appl. Catal., B*, 2020, **278**, 119339.

131 C. Wang, Y. Wu, A. Bodach, M. L. Krebs, W. Schuhmann and F. Schüth, A novel electrode for value-generating anode reactions in water electrolyzers at industrial current densities, *Angew. Chem., Int. Ed.*, 2023, **62**, e202215804.

132 J. N. Hausmann, R. Beltrán-Suito, S. Mebs, V. Hlukhyy, T. F. Fässler, H. Dau, M. Driess and P. W. Menezes, Evolving highly active oxidic iron(III) phase from corrosion of intermetallic iron silicide to master efficient electrocatalytic water oxidation and selective oxygenation of 5-hydroxymethylfurfural, *Adv. Mater.*, 2021, **33**, 2008823.

133 M. Braun, M. Chatwani, P. Kumar, Y. Hao, I. Sanjuán, A.-A. Apostolieri, A. C. Brix, D. M. Morales, U. Hagemann, M.



Heidelmann, J. Masa, W. Schuhmann and C. Andronescu, Cobalt nickel boride as electrocatalyst for the oxidation of alcohols in alkaline media, *JPhys Energy*, 2023, **5**, 024005.

134 A. C. Brix, D. M. Morales, M. Braun, D. Jambrec, J. R. C. Junqueira, S. Cychy, S. Seisel, J. Masa, M. Muhler, C. Andronescu and W. Schuhmann, Electrocatalytic oxidation of glycerol using solid-state synthesised nickel boride: Impact of key electrolysis parameters on product selectivity, *ChemElectroChem*, 2021, **8**, 2336–2342.

135 N. P. Kocatürk-Schumacher, J. Madjarov, P. Viwatthanasittiphong and S. Kerzenmacher, Toward an energy efficient wastewater treatment: Combining a microbial fuel cell/electrolysis cell anode with an anaerobic membrane bioreactor, *Front. Energy Res.*, 2018, **6**, 95.

136 S. Colantoni, Ó. Santiago, J. R. Weiler, M. T. Knoll, C. J. Lapp, J. Gescher and S. Kerzenmacher, Comparative study of bioanodes for microbial electrolysis cells operation in anaerobic digester conditions, *J. Environ. Chem. Eng.*, 2024, **12**, 113071.

137 S. Palkovits and R. Palkovits, The role of electrochemistry in future dynamic bio-refineries: A focus on (non-)Kolbe electrolysis, *Chem. Ing. Tech.*, 2019, **91**, 699–706.

138 C. Urban, J. Xu, H. Sträuber, T. R. d. S. Dantas, J. Mühlberg, C. Härtig, L. T. Angenent and F. Harnisch, Production of drop-in fuels from biomass at high selectivity by combined microbial and electrochemical conversion, *Energy Environ. Sci.*, 2017, **10**, 2231–2244.

139 L. F. M. Rosa, K. Röhrling and F. Harnisch, Electrolysis of medium chain carboxylic acids to aviation fuel at technical scale, *Fuel*, 2024, **356**, 129590.

140 K. Neubert, M. Hell, M. C. Morejón and F. Harnisch, Hetero-coupling of bio-based medium-chain carboxylic acids by Kolbe electrolysis enables high fuel yield and efficiency, *ChemSusChem*, 2022, **15**, e202201426.

141 A. Manzotti, M. J. Robson and F. Ciucci, Recent developments in membraneless electrolysis, *Curr. Opin. Green Sustainable Chem.*, 2023, **40**, 100765.

142 A. Hodges, A. L. Hoang, G. Tsekouras, K. Wagner, C.-Y. Lee, G. F. Swiegers and G. G. Wallace, A high-performance capillary-fed electrolysis cell promises more cost-competitive renewable hydrogen, *Nat. Commun.*, 2022, **13**, 1304.

143 J.-T. Ren, L. Chen, H.-Y. Wang, W.-W. Tian and Z.-Y. Yuan, Water electrolysis for hydrogen production: from hybrid systems to self-powered/catalyzed devices, *Energy Environ. Sci.*, 2024, **17**, 49–113.

144 A. C. Blaga, A. Tucaliuc and L. Kloetzer, Applications of ionic liquids in carboxylic acids separation, *Membranes*, 2022, **12**, 771.

145 E. M. Karp, R. M. Cywar, L. P. Manker, P. O. Saboe, C. T. Nimlos, D. Salvachúa, X. Wang, B. A. Black, M. L. Reed, W. E. Michener, N. A. Rorrer and G. T. Beckham, Post-fermentation recovery of biobased carboxylic acids, *ACS Sustainable Chem. Eng.*, 2018, **6**, 15273–15283.

146 C. Huang, T. Xu, Y. Zhang, Y. Xue and G. Chen, Application of electrodialysis to the production of organic acids: State-of-the-art and recent developments, *J. Membr. Sci.*, 2007, **288**, 1–12.

147 S. Tönjes, E. Uitterhaegen, K. De Winter and W. Soetaert, Reactive extraction technologies for organic acids in industrial fermentation processes – A review, *Sep. Purif. Technol.*, 2025, **356**, 129881.

148 Y. S. Aşçı, Examination of the efficiency of ionic liquids in glycolic acid separation from aqueous solution by using reactive extraction method, *J. Turk. Chem. Soc., Sect. A*, 2017, **4**, 981–992.

149 K. Wasewar, Reactive extraction: An intensifying approach for carboxylic acid separation, *Int. J. Chem. Eng. Appl.*, 2012, **3**, 249–255.

150 L. Handojo, A. K. Wardani, D. Regina, C. Bella, M. T. A. P. Kresnowati and I. G. Wenten, Electro-membrane processes for organic acid recovery, *RSC Adv.*, 2019, **9**, 7854–7869.

151 Q. Wang, G. Q. Chen, L. Lin, X. Li and S. E. Kentish, Purification of organic acids using electrodialysis with bipolar membranes (EDBM) combined with monovalent anion selective membranes, *Sep. Purif. Technol.*, 2021, **279**, 119739.

152 Z. Wang, J. Yan, H. Wang, W. Fu, D. He, B. Wang, Y. Wang and T. Xu, Separation and conversion of CO₂ reduction products into high-concentration formic acid using bipolar membrane electrodialysis, *J. Membr. Sci.*, 2024, **708**, 123016.

153 Z. Teimouri, N. Abatzoglou and A. K. Dalai, Kinetics and selectivity study of Fischer-Tropsch synthesis to C5+ hydrocarbons: A Review, *Catalysts*, 2021, **11**, 330.

154 M. Martinelli, M. K. Gnanamani, S. LeViness, G. Jacobs and W. D. Shafer, An overview of Fischer-Tropsch Synthesis: XTL processes, catalysts and reactors, *Appl. Catal., A*, 2020, **608**, 117740.

155 Y. Yang and F. Li, Reactor design for electrochemical CO₂ conversion toward large-scale applications, *Curr. Opin. Green Sustainable Chem.*, 2021, **27**, 100419.

156 C. M. Gabardo, C. P. O'Brien, J. P. Edwards, C. McCallum, Y. Xu, C.-T. Dinh, J. Li, E. H. Sargent and D. Sinton, Continuous carbon dioxide electroreduction to concentrated multi-carbon products using a membrane electrode assembly, *Joule*, 2019, **3**, 2777–2791.

157 L. Han, W. Zhou and C. Xiang, High-rate electrochemical reduction of carbon monoxide to ethylene using Cu nanoparticle-based gas diffusion electrodes, *ACS Energy Lett.*, 2018, **3**, 855–860.

158 M. B. C. de Souza, K.-E. Guima, P. S. Fernández and C. A. Martins, Glycerol is converted into energy and carbonyl compounds in a 3d-printed microfluidic fuel cell: In situ and in operando Bi-modified Pt anodes, *ACS Appl. Mater. Interfaces*, 2022, **14**, 25457–25465.

159 R. Phillips, A. Edwards, B. Rome, D. R. Jones and C. W. Dunnill, Minimising the ohmic resistance of an alkaline electrolysis cell through effective cell design, *Int. J. Hydrogen Energy*, 2017, **42**, 23986–23994.

160 S. Jeong, T. Ohto, T. Nishiuchi, Y. Nagata, J. Fujita and Y. Ito, Suppression of methanol and formate crossover



through sulfanilic-functionalized holey graphene as proton exchange membranes, *Adv. Sci.*, 2023, **10**, 2304082.

161 E. Antolini and E. R. Gonzalez, Alkaline direct alcohol fuel cells, *J. Power Sources*, 2010, **195**, 3431–3450.

162 H. Becker, J. Murawski, D. V. Shinde, I. E. L. Stephens, G. Hinds and G. Smith, Impact of impurities on water electrolysis: a review, *Sustainable Energy Fuels*, 2023, **7**, 1565–1603.

163 R. M. El-Zoheiry, S. Ookawara and M. Ahmed, Efficient fuel utilization by enhancing the under-rib mass transport using new serpentine flow field designs of direct methanol fuel cells, *Energy Convers. Manage.*, 2017, **144**, 88–103.

164 C. Daoudi and T. Bounahmidi, Overview of alkaline water electrolysis modeling, *Int. J. Hydrogen Energy*, 2024, **49**, 646–667.

165 A. Pezzini, U. J. de Castro, D. S. B. L. de Oliveira, G. Tremiliosi-Filho and R. de Sousa Júnior, Mathematical modeling of alkaline direct glycerol fuel cells, *Energies*, 2023, **16**, 6762.

